REPORT

Bi-allelic *DNAH8* Variants Lead to Multiple Morphological Abnormalities of the Sperm Flagella and Primary Male Infertility

Chunyu Liu,[1,2,3,20] Haruhiko Miyata,[4,20] Yang Gao,[5,6,7,20] Yanwei Sha,[8,9,20] Shuyan Tang,[1,2,20] Zoulan Xu,[4,10,20] Marjorie Whitfield,[11,12,13] Catherine Patrat,[11,12,13,14] Huan Wu,[5,6,7] Emmanuel Dulioust,[11,12,13,14] Shixiong Tian,[1,2] Keisuke Shimada,[4] Jiangshan Cong,[1,2] Taichi Noda,[4] Hang Li,[5,6,7] Akane Morohoshi,[4,15] Caroline Cazin,[16,17,18] Zine-Eddine Kherraf,[16,17] Christophe Arnoult,[16] Li Jin,[1] Xiaojin He,[5,6,7] Pierre F. Ray,[16,17,21] Yunxia Cao,[5,6,7,21] Aminata Touré,[11,12,13,21] Feng Zhang,[1,2,3,21,*] and Masahito Ikawa[4,10,15,19,21,*]

Sperm malformation is a direct factor for male infertility. Multiple morphological abnormalities of the flagella (MMAF), a severe form of asthenoteratozoospermia, are characterized by immotile spermatozoa with malformed and/or absent flagella in the ejaculate. Previous studies indicated genetic heterogeneity in MMAF. To further define genetic factors underlying MMAF, we performed whole-exome sequencing in a cohort of 90 Chinese MMAF-affected men. Two cases (2.2%) were identified as carrying bi-allelic missense *DNAH8* variants, variants which were either absent or rare in the control human population and were predicted to be deleterious by multiple bioinformatic tools. Re-analysis of exome data from a second cohort of 167 MMAF-affected men from France, Iran, and North Africa permitted the identification of an additional male carrying a *DNAH8* homozygous frameshift variant. *DNAH8* encodes a dynein axonemal heavy-chain component that is expressed preferentially in the testis. Hematoxylin-eosin staining and electron microscopy analyses of the spermatozoa from men harboring bi-allelic *DNAH8* variants showed a highly aberrant morphology and ultrastructure of the sperm flagella. Immunofluorescence assays performed on the spermatozoa from men harboring bi-allelic *DNAH8* variants revealed the absent or markedly reduced staining of DNAH8 and its associated protein DNAH17. *Dnah8*-knockout male mice also presented typical MMAF phenotypes and sterility. Interestingly, intracytoplasmic sperm injections using the spermatozoa from *Dnah8*-knockout male mice resulted in good pregnancy outcomes. Collectively, our experimental observations from humans and mice demonstrate that DNAH8 is essential for sperm flagellar formation and that bi-allelic deleterious *DNAH8* variants lead to male infertility with MMAF.

Human infertility, defined as the inability to achieve a clinical pregnancy despite 12 months of regular and unprotected intercourse, has become a widespread health issue.[1] Multiple morphological abnormalities of the flagella (MMAF) are defined by the combination of absent, short, bent, coiled, and/or irregular-caliber flagella.[2] Previous genetic studies revealed a series of MMAF-associated genes in cases of primary infertility without primary ciliary dyskinesia (PCD; MIM: 244400) associated symptoms (reviewed by Touré et al.).[3–14] However, these genetic findings account for approximately 35% to 60% of MMAF cases,[11,12] demonstrating the high genetic heterogeneity of this disorder and the necessity for further genetic explorations.

Cilia and flagella are hair-like organelles extending from the cell surface.[15,16] Both contain an important core component, termed the axoneme, which is an evolutionarily conserved structure consisting of a highly ordered "9 + 2" arrangement of nine peripheral microtubule doublets and two central microtubules.[17] A number of multiprotein complexes (including radial spokes, nexin-dynein regulatory complex, central complex, and dynein arms)

[1]Obstetrics and Gynecology Hospital, NHC Key Laboratory of Reproduction Regulation (Shanghai Institute of Planned Parenthood Research), State Key Laboratory of Genetic Engineering at School of Life Sciences, Fudan University, Shanghai 200011, China; [2]Shanghai Key Laboratory of Female Reproductive Endocrine Related Diseases, Shanghai 200011, China; [3]State Key Laboratory of Reproductive Medicine, Center for Global Health, School of Public Health, Nanjing Medical University, Nanjing 211116, China; [4]Research Institute for Microbial Diseases, Osaka University, Osaka 565-0871, Japan; [5]Reproductive Medicine Center, Department of Obstetrics and Gynecology, The First Affiliated Hospital of Anhui Medical University, Hefei 230022, China; [6]NHC Key Laboratory of Study on Abnormal Gametes and Reproductive Tract, Anhui Medical University, Hefei 230032, China; [7]Key Laboratory of Population Health Across Life Cycle, Anhui Medical University, Ministry of Education of the People's Republic of China, Hefei 230032, China; [8]Department of Andrology, United Diagnostic and Research Center for Clinical Genetics, School of Public Health & Women and Children's Hospital, Xiamen University, Xiamen 361005, Fujian, China; [9]State Key Laboratory of Molecular Vaccinology and Molecular Diagnostics & Center for Molecular Imaging and Translational Medicine, School of Public Health, Xiamen University, Xiamen 361102, China; [10]Graduate School of Pharmaceutical Sciences, Osaka University, Osaka 565-0871, Japan; [11]INSERM U1016, Institut Cochin, Paris 75014, France; [12]Centre National de la Recherche Scientifique UMR8104, Paris 75014, France; [13]Faculté de Médecine, Université de Paris, Paris 75014, France; [14]Laboratoire d'Histologie Embryologie—Biologie de la Reproduction—CECOS Groupe Hospitalier Universitaire Paris Centre, Assistance Publique-Hôpitaux de Paris, Paris 75014, France; [15]Graduate School of Medicine, Osaka University, Osaka 565-0871, Japan; [16]Team Genetics Epigenetics and Therapies of Infertility, Institute for Advanced Biosciences, Grenoble Alpes University (UGA), INSERM U1209, Centre National de la Recherche Scientifique UMR 5309, Grenoble 38000, France; [17]UM de genetique de l'infertilite et de diagnostic pre-implantatoire (GI-DPI), Centre Hospitalier Universitaire Grenoble Alpes (CHUGA), Grenoble 38000, France; [18]Service de Génétique, Laboratoire Eurofins Biomnis, Lyon, France; [19]Institute of Medical Science, University of Tokyo, Tokyo 108-8639, Japan
[20]These authors contributed equally to this work
[21]These authors contributed equally to this work
*Correspondence: zhangfeng@fudan.edu.cn (F.Z.), ikawa@biken.osaka-u.ac.jp (M.I.)
https://doi.org/10.1016/j.ajhg.2020.06.004.

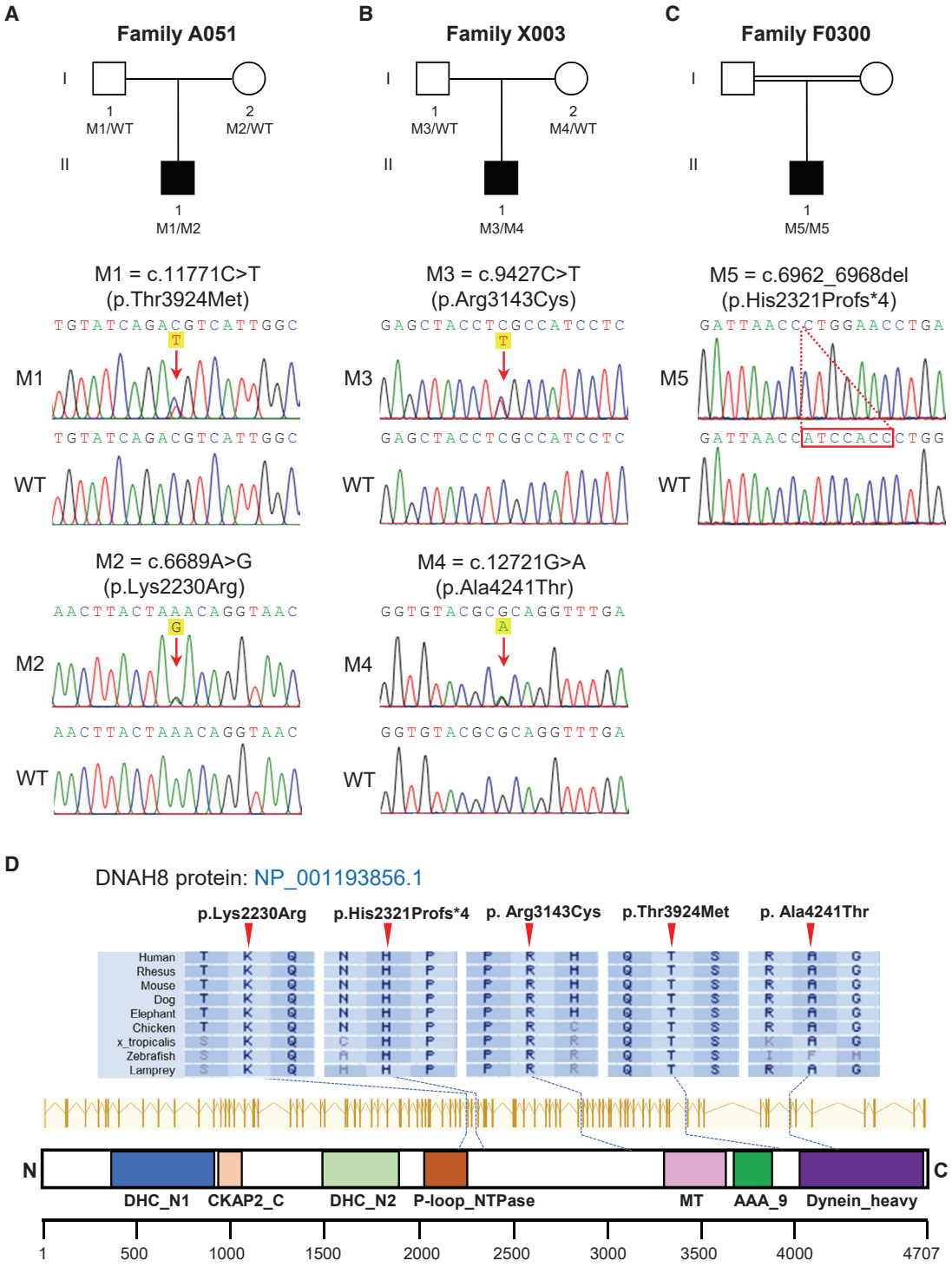

Figure 1. Identification of Bi-allelic *DNAH8* Variants in Men with MMAF

(A–C) The pedigrees of three families affected by *DNAH8* variants. The NCBI reference sequence number for *DNAH8* transcript is NM_001206927.2. Sanger sequencing results are shown below the pedigrees. The variant positions are indicated by red arrows or a dashed box. WT, wild type.

(D) Variant locations and phylogenetic conservation of the mutated residues in DNAH8 protein. The NCBI reference sequence number for DNAH8 protein is NP_001193856.1. Colored squares denote different domains according to the NCBI browser. DHC_N1—dynein heavy chain, N-terminal region 1; CKAP2_C—cytoskeleton-associated protein 2 C terminus; DHC_N2—dynein heavy chain, N-terminal region 2; P-loop_NTPase—P-loop containing nucleoside triphosphate hydrolases; MT—microtubule-binding stalk of dynein motor; AAA_9—ATP-binding dynein motor region D5; Dynein_heavy—dynein heavy chain and region D6 of dynein motor.

Table 1. Bi-allelic *DNAH8* Variants Identified in MMAF-affected Men

-	Subject A051		Subject X003		Subject F0300
cDNA alteration	c.11771C>T	c.6689A>G	c.9427C>T	c.12721G>A	c.6962_6968del
Variant allele	heterozygous	heterozygous	heterozygous	heterozygous	homozygous
Protein alteration	p.Thr3924Met	p.Lys2230Arg	p.Arg3143Cys	p.Ala4241Thr	p.His2321Profs*4
Variant type	missense	missense	missense	missense	frameshift
Allele Frequency in Human Population					
1000 Genomes	0	0	0	0	0
gnomAD (v3)	0.006729	0	0.0004677	0.0001187	0
Function Prediction					
SIFT	damaging	damaging	damaging	damaging	NA
PolyPhen-2	damaging	damaging	damaging	damaging	NA
MutationTaster	damaging	damaging	damaging	damaging	damaging

NCBI reference sequence number of *DNAH8* is NM_001206927.2.
NA, not applicable.

constitute the major components of the axoneme.[18] Among the complexes, the outer and inner dynein arms (ODAs and IDAs, respectively) play an important role in the beating of cilia and flagella through ATP hydrolysis.[19] Previous studies have revealed that mutations in IDA and ODA protein complexes cause several ciliopathies and male infertility. In particular, the deficiency of *DNAH1* (MIM: 603332), which encodes an important component of the IDA heavy chain, leads to isolated male infertility with MMAF.[2] Importantly, recent studies reported that mutations in *DNAH17* (MIM: 610063; encoding a sperm-specific ODA heavy-chain component) also cause isolated male infertility due to asthenoteratozoospermia.[13,20] These findings suggest the potential involvement of other components of dynein arms in male infertility and sperm flagellar malformations.

Here, two distinct MMAF cohorts were analyzed. The first cohort comprised 90 Chinese MMAF-affected men enrolled from the First Affiliated Hospital of Anhui Medical University and the Women and Children's Hospital of Xiamen University in China. The second cohort comprised 167 individuals with MMAF, including 83 men from North Africa (Algeria, Libya, and Tunisia; enrolled at the Clinique des Jasmins in Tunis), 52 men recruited at the Royan Institute (Reproductive Biomedicine Research Center) in Iran, and 32 men recruited in France (mainly at the

Table 2. Semen Characteristics and Sperm Flagellar Morphology of Men Carrying Bi-allelic *DNAH8* Variants

-	Subject A051	Subject X003	Subject F0300	Reference Values
Semen Parameters				
Semen volume (mL)	2.2	3.2	7.1	>1.5
Sperm concentration (10^6/mL)	39.1	42.7	13.6*	>15.0
Total sperm count (10^6)	86.0	136.7	96.6	>39.0
Motility (%)	4.0*	2.7*	8.0*	>40.0
Progressive motility (%)	1.3*	1.5*	4.0*	>32.0
Sperm Flagellar Morphology				
Absent flagella (%)	2.0	2.5	4.0	<5.0
Short flagella (%)	7.1*	9.0*	8.0*	<1.0
Coiled flagella (%)	57.1*	32.0*	33.0*	<17.0
Angulation (%)	0.5	6.0	19.0*	<13.0
Irregular caliber (%)	1.0	26.0*	8.0*	<2.0
Normal flagella (%)	32.3	24.5	28.0	>23.0

Lower and upper reference limits are shown according to the World Health Organization standards[46] and the distribution ranges of morphologically abnormal spermatozoa observed in fertile individuals.[47]
*Abnormal values.

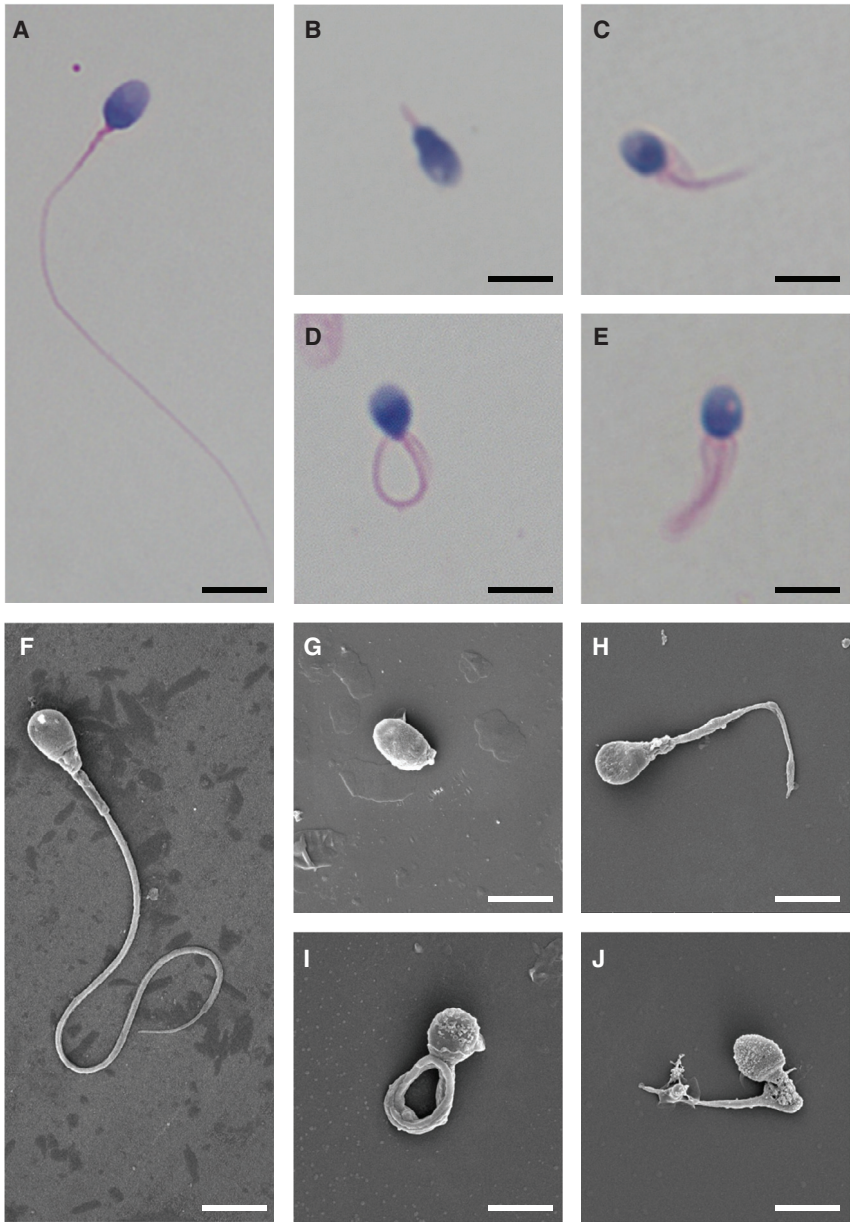

Figure 2. Morphology of the Spermatozoa from Men Harboring Bi-allelic *DNAH8* Variants

(A) Normal morphology of the spermatozoon from a healthy control male evident under light microscopy. Scale bars: 5 μm.

(B–E) Most spermatozoa from men harboring bi-allelic *DNAH8* variants presented MMAF phenotypes, including absent (B), short (C), coiled (D), and irregular-caliberflagella (E). The data of subject A051 as an example.

(F) Normal morphology of the spermatozoon from a healthy control male as revealed by scanning electronic microscopy.

(G–J) The MMAF phenotypes, including absent (G), short (H), coiled (I), irregular-caliber flagella (J), were clearly revealed in the spermatozoa from subject A051 harboring bi-allelic *DNAH8* variants.

Reproductive Department of the Cochin Hospital in Paris). The clinical phenotypes of the affected individuals are summarized in the Supplemental Note (see Supplemental Information). Informed consent was obtained from all subjects participating in the study. The study regarding the cohorts was approved by the institutional review boards at all of the participating institutes.

To investigate the unknown genetic factors involved in human MMAF, we performed whole-exome sequencing (WES) analyses in the first cohort of 90 Chinese men with MMAF. After applying stringent bioinformatic analyses according to our previously described protocol,[4] we identified two men (2.2%) harboring bi-allelic missense variants in *DNAH8* (MIM: 603337; NCBI: NM_001206927.2). The *DNAH8*-mutated alleles were c.11771C>T (p.Thr3924Met) plus c.6689A>G (p.Lys2230Arg) in subject A051 (II-1 in Figure 1A) and c.9427C>T (p.Arg3143Cys) plus c.12721G>A (p.Ala4241Thr) in subject X003 (II-1 in Figure 1B). Subsequent Sanger sequencing confirmed that these bi-allelic *DNAH8* variants were inherited from heterozygous parental carriers (Figures 1A and 1B; Table S1). All of the *DNAH8* variants were either absent or rare in the human genome datasets archived in the 1000 Genomes Project and gnomAD databases. These *DNAH8* variants were also predicted to be damaging through the use of the PolyPhen-2, SIFT, and MutationTaster tools (Table 1).

WES analysis of the 167 MMAF-affected men from the second cohort identified an additional case in an individual of Moroccan ancestry (Figure 1C). This MMAF-affected subject F0300 (II-1 in Figure 1C) harbored a homozygous frameshift variant (c.6962_6968del [p.His2321Profs*4]) that produced a frameshift and premature stop codon in *DNAH8*. No DNA was available from family members of subject F0300. His brother was reported to be infertile, although no further investigation could be performed. We note that his parents are consanguineous, thus strongly supporting the likelihood that this *DNAH8* frameshift variant was also transmitted under a recessive mode of inheritance.

Importantly, the residues in DNAH8 affected by these aforementioned variants are all highly conserved across species (Figure 1D). Furthermore, no bi-allelic deleterious variants in previously described MMAF- or PCD-associated genes were observed in the three men with bi-allelic *DNAH8* variants. These findings further suggest that the infertility phenotypes were likely caused by the identified bi-allelic *DNAH8* variants.

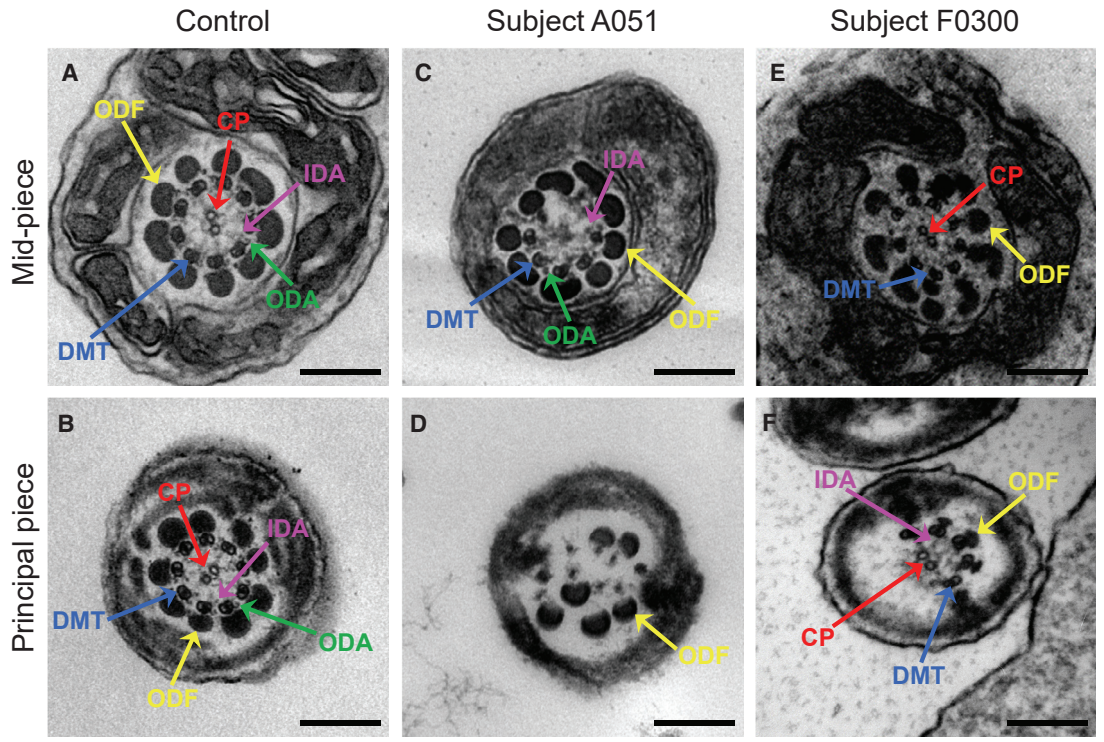

Figure 3. TEM Analyses of Sperm Cells from Men Harboring Bi-allelic *DNAH8* Variants
(A and B) Cross-sections of the mid-piece (A) and principal piece (B) of the sperm flagella in a control individual show the typical "9 + 2" microtubule structure, including nine pairs of peripheral microtubule doublets (DMT; blue arrows), nine outer dense fibers (ODF; yellow arrows), and the central pair of microtubules (CP; red arrows). The outer dynein arms (ODA; green arrows) and inner dynein arms (IDA; pink arrows) are also visible. Scale bars: 200 μm.
(C–F) In the spermatozoa from men harboring bi-allelic *DNAH8* variants, various axonemal anomalies can be observed, including the lack of CP (C) or DMT (D). Misarranged (D) or supernumerary ODFs (E) were also observed. ODAs were disassembled or absent in the samples from men carrying bi-allelic *DNAH8* variants (C–F).

DNAH8 contains 92 exons and encodes a predicted 4,707-amino-acid protein (NCBI: NP_001193856.1; UniProt: A0A075B6F3). The DNAH8 protein is preferentially expressed in the human testis, according to the Human Protein Atlas. Our reverse transcription polymerase chain reaction (RT-PCR) assays also indicated that mouse *Dnah8* is predominantly expressed in the testis (Figure S1A). Furthermore, the expression of mouse *Dnah8* mRNA in the testis began at 14 days after birth, corresponding to the pachytene stage (Figure S1B).

Semen parameters of men harboring bi-allelic *DNAH8* variants were analyzed in the source laboratories according to World Health Organization guidelines.[21] Sperm motility and progressive motility in the men harboring bi-allelic *DNAH8* variants were dramatically lower than the normal reference values (Table 2). Hematoxylin-eosin (H&E) staining and scanning electron microscopy examination were performed to assess sperm morphology. Approximately 70% of the immotile spermatozoa displayed abnormal flagella, including absent, short, and coiled flagella, angulation, and irregular caliber (Figure 2 and Table 2).

Various ultrastructural defects were revealed by transmission electron microscopy (TEM) in the sperm flagella from men harboring bi-allelic *DNAH8* variants. The typical "9 + 2" microtubule structure was observed in the spermatozoa from control men (Figure 3). However, a dramatic disorganization in axonemal or peri-axonemal structures (including disorganized peripheral microtubule doublets and outer dense fibers, missing or disassembled ODAs, and absent central pairs) was detected in the spermatozoa from men harboring bi-allelic *DNAH8* variants (Figure 3). Quantification conducted on transverse sections of the sperm flagella indicated higher rates of abnormal flagellar ultrastructure in men harboring bi-allelic *DNAH8* variants than those in the normal control (Table S2).

To further investigate the pathogenicity of bi-allelic *DNAH8* variants, we analyzed the levels of *DNAH8* mRNA and DNAH8 protein using RT-PCR (Table S3) and immunofluorescence assays, respectively. The abundance of *DNAH8* mRNA in the sperm from subject A051, who harbored bi-allelic *DNAH8* variants, was significantly reduced when compared to the normal control (Figure S2). As for the protein level, in the normal control man, DNAH8 immunostaining was concentrated along the mid-piece and principal piece of the sperm flagella (Figure S3). This observation in humans is consistent with previous evidence in wild-type male mice.[22] In contrast, DNAH8 immunostaining was almost absent in

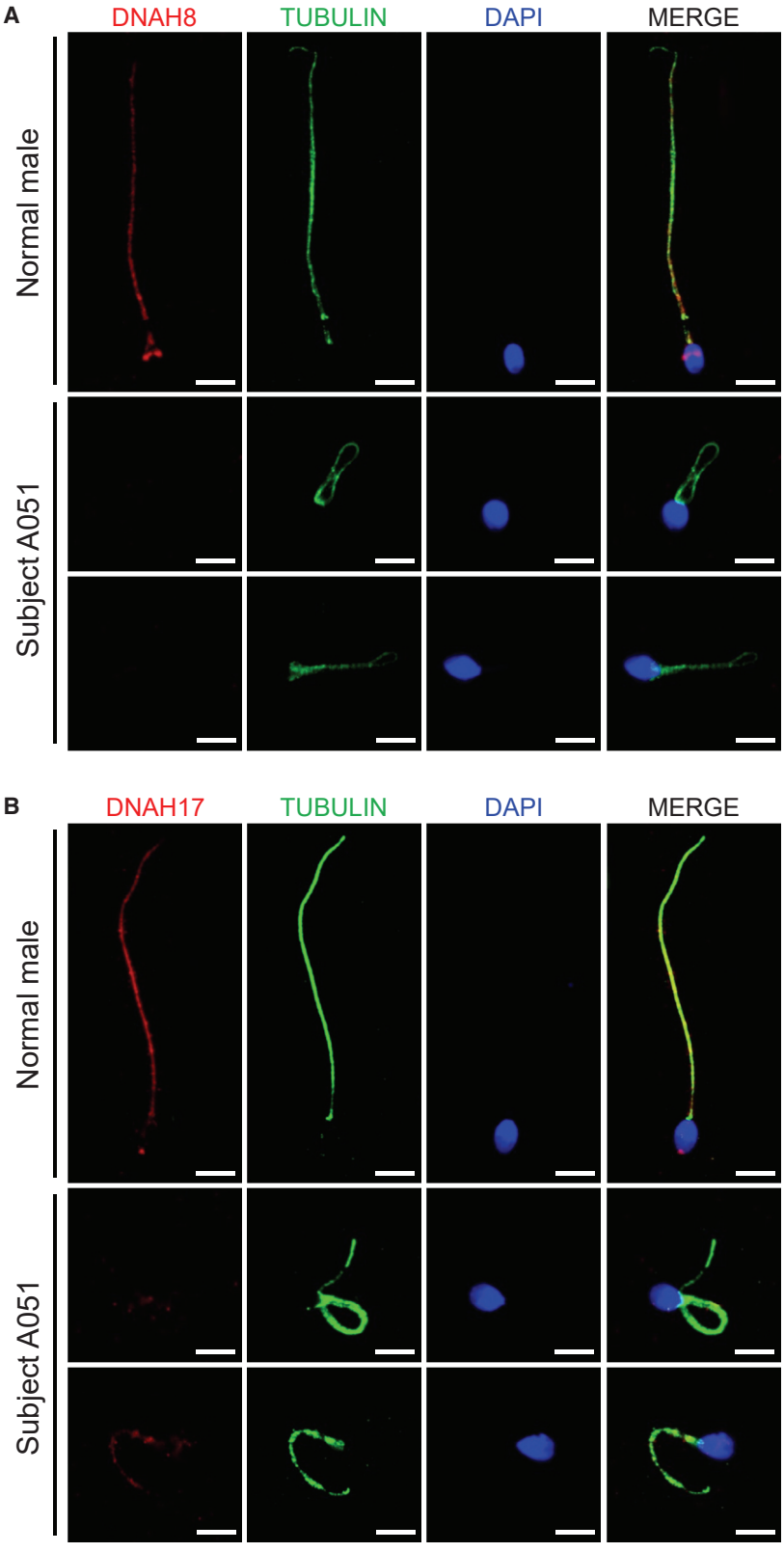

Figure 4. Localization of DNAH8 and Associated Protein DNAH17 in the Spermatozoa from Men Harboring Bi-allelic *DNAH8* Variants
(A) Immunofluorescence staining of the spermatozoa from a normal control male and subjects carrying bi-allelic *DNAH8* variants. Anti-DNAH8 (red) and anti-α-tubulin (green) antibodies were used. Spermatozoa were counterstained with 4′,6-diamidino-2-phenylindole as a marker of the cell nucleus. In the fertile control male, DNAH8 immunostaining (red) concentrated along the sperm flagella, but this signal was almost absent from the sperm flagella from subjects harboring bi-allelic *DNAH8* variants. The data of subject A051 are provided to illustrate the typical staining observed in the *DNAH8*-associated cases. Scale bars: 5 μm.
(B) DNAH17 immunostaining is affected in the spermatozoa from men harboring bi-allelic *DNAH8* variants. The spermatozoa were stained with anti-DNAH17 (red) and anti-α-tubulin (green) antibodies. DNAH17 staining mainly localized along the spermflagella from a control male, while being evidently reduced in the spermatozoa from subject A051. Scale bars: 5 μm.

the sperm flagella from all three subjects harboring bi-allelic *DNAH8* variants, including both missense and frameshift variants (Figure 4A and Figure S3A). We also examined the presence of DNAH17, which is required for accurate localization of DNAH8.[13] Notably, the staining of DNAH17 was dramatically reduced in the spermatozoa from men harboring bi-allelic *DNAH8* variants (Figure 4B and Figure S3B).

DNAH8 is highly conserved among different species during evolution. Consistent with the human data available from the Human Protein Atlas, the murine ortholog *Dnah8* is also preferentially expressed in the testis, as per our RT-PCR assays conducted in a set of various mouse tissues (Figure S1, Table S4). To further investigate the role of mouse *Dnah8* in sperm flagellar formation, we generated *Dnah8*-knockout (KO; $Dnah8^{em1/em1}$) mice through the use of CRISPR-Cas9 technology. Two guide RNAs targeting the regions near the start and stop codons were used to delete the entire coding region of *Dnah8* (Figure S4A). Polymerase chain reaction (PCR) and Sanger sequencing were performed to confirm the mutated allele in *Dnah8*-KO mice (Figures S4B and S4C). We also used an immunoblot assay to investigate the level of DNAH8 protein in the testes of wild-type and *Dnah8*-KO male mice. As shown in Figure S5, the signal of DNAH8 was absent in the testis from *Dnah8*-KO male mice. No significant differences were observed in testis weight between *Dnah8*-KO and heterozygous mutated male mice (Figure S6).

Sperm parameters and morphology of *Dnah8*-KO male mice were also investigated. As shown in Table 3, Video S1, and Video S2, diminished sperm movement was

Table 3. Sperm Characteristics and Flagellar Morphology of *Dnah8*-KO Male Mice

-	Heterozygous Control (*Dnah8*$^{wt/em1}$)	KO (*Dnah8*$^{em1/em1}$)
Semen Parameter		
Motility (%)	91.7 ± 1.5	0 ± 0***
Sperm Flagellar Morphology[a]		
Absent flagella (%)	4.0 ± 2.6	18.5 ± 17.8*
Short flagella (%)	0.0 ± 0.0	25.7 ± 1.2***
Coiled flagella (%)	0.0 ± 0.0	25.5 ± 15.6**
Irregular caliber (%)	0.2 ± 0.3	20.5 ± 12.6***
Bent flagella (%)	0.7 ± 0.8	9.8 ± 1.6***

[a]Data represent the mean ± SD of three independent experiments.
*$p < 0.05$, **$p < 0.01$, ***$p < 0.001$.

observed in *Dnah8*-KO male mice when compared to heterozygous mutated (*Dnah8*$^{wt/em1}$) male mice. H&E staining revealed significantly higher rates of abnormal flagella in *Dnah8*-KO male mice than those in heterozygous mutated male mice (Table 3 and Figure 5A). The sperm flagella of *Dnah8*-KO male mice also presented with absent, short, coiled, bent, and/or irregular shapes, which recapitulated the clinical phenotypes of MMAF-affected men with bi-allelic *DNAH8* variants. Furthermore, TEM analysis of sperm flagella showed disorganized microtubules and outer dense fibers in the spermatozoa from *Dnah8*-KO male mice (Figure 5B). These experimental observations on *Dnah8*-KO male mice conclusively demonstrated the crucial role of DNAH8 in sperm flagellar formation.

To further investigate the role of DNAH8 in spermatogenesis, we performed H&E staining on the testes of *Dnah8*-KO and heterozygous mutated male mice (Figure 6A). In stage VII–VIII seminiferous tubules, no elongated tails were observed in the testes from *Dnah8*-KO male mice, but normal round spermatids were observed, indicating the involvement of DNAH8 in sperm flagellar formation. Periodic acid–Schiff (PAS) staining of the cauda epididymis from *Dnah8*-KO male mice displayed fewer sperm heads than did those from heterozygous mutated mice (Figure 6B). Collectively, these data suggest that DNAH8 deficiency can result in MMAF and male infertility in both humans and mice.

To assess the fertility and reproductive behavior of *Dnah8*-KO male mice, sexually mature *Dnah8*-KO and heterozygous mutated male mice were individually caged with 8-week-old wild-type B6D2F1 female mice (one male with three females) for 2 months, and plugs were checked every morning. Pups were counted on the day of birth. As shown in Figure S7, normal mounting and copulatory plugs were observed for both groups of *Dnah8*-KO and heterozygous mutated male mice. However, *Dnah8*-KO male mice failed to produce any offspring over 2 months of breeding, whereas heterozygous mutated males routinely produced offspring (Figure S7). These experimental observations indicate that DNAH8 is necessary for male fertility in mice.

Intracytoplasmic sperm injection (ICSI) has been reported to be efficient for most MMAF-associated asthenoteratozoospermia.[23] To examine whether *DNAH8*-associated male infertility could also be overcome via ICSI, we conducted experiments using the sperm from wild-type and *Dnah8*-KO male mice. As shown in Figure 7, pups were successfully obtained upon ICSI using the spermatozoa from *Dnah8*-KO male mice after the transfer of two-cell embryos to pseudopregnant ICR females. Genotyping assays confirmed that all these pups were heterozygous *Dnah8*-mutated carriers, as anticipated. Our findings indicated that *Dnah8*-associated KO male infertility in mice could be overcome by ICSI. Consistent with these experimental observations, the second ICSI attempt performed using the sperm from subject F0300 (who harbored a homozygous *DNAH8* frameshift variant) was successful and resulted in a live birth. Overall, our data strongly suggest that ICSI could serve as a promising treatment for infertile men harboring bi-allelic *DNAH8* variants.

As highly conserved beating organelles, motile cilia and flagella are required for cell motility and signaling.[24] The axonemal ultrastructure, which is shared by cilia and flagella, consists of a circle of nine peripheral microtubule doublets arranged around a central pair of microtubules.[17] Distinct multi-protein dynein complexes, which are attached regularly to peripheral microtubule doublets, contain molecular motors that can generate microtubule sliding and thus regulate the movement of motile cilia and flagella.[19]

The mammalian ODA is a complex structure that is attached to the peripheral microtubules via a docking complex. It is responsible for ciliary and flagellar beating.[25–27] Previous studies reported two types of human ODAs. In airway epithelial cells, type 1 ODAs (e.g., DNAH11) reside in the proximal part of the cilium, whereas type 2 ODAs (e.g., DNAH9) reside in the distal part of the cilium.[28,29] The deficiency of ODA-associated proteins results in PCD and/or asthenoteratozoospermia. For example, disruptions in DNAH5 and DNAH11 are associated with PCD.[28,30] Furthermore, mutations in *DNAH9* (MIM: 603330), *DNAI1* (MIM: 604366), and *DNAI2* (MIM: 605483) induce PCD and male infertility.[18,31,32] These previous observations indicate the important roles of ODA-associated proteins in ciliary and flagellar morphology and motility.

Here, our genetic analyses using WES on two distinct cohorts with MMAF (in total, 257 cases) identified three (1.2%) unrelated men carrying bi-allelic variants in *DNAH8*, which encodes an ODA heavy chain component of the axoneme that is preferentially expressed in the testis. These *DNAH8* variants are either rare or absent in human populations, but they were enriched in the MMAF-affected cases of different ancestries, indicating that *DNAH8* deficiency could be another important cause of MMAF across human populations.

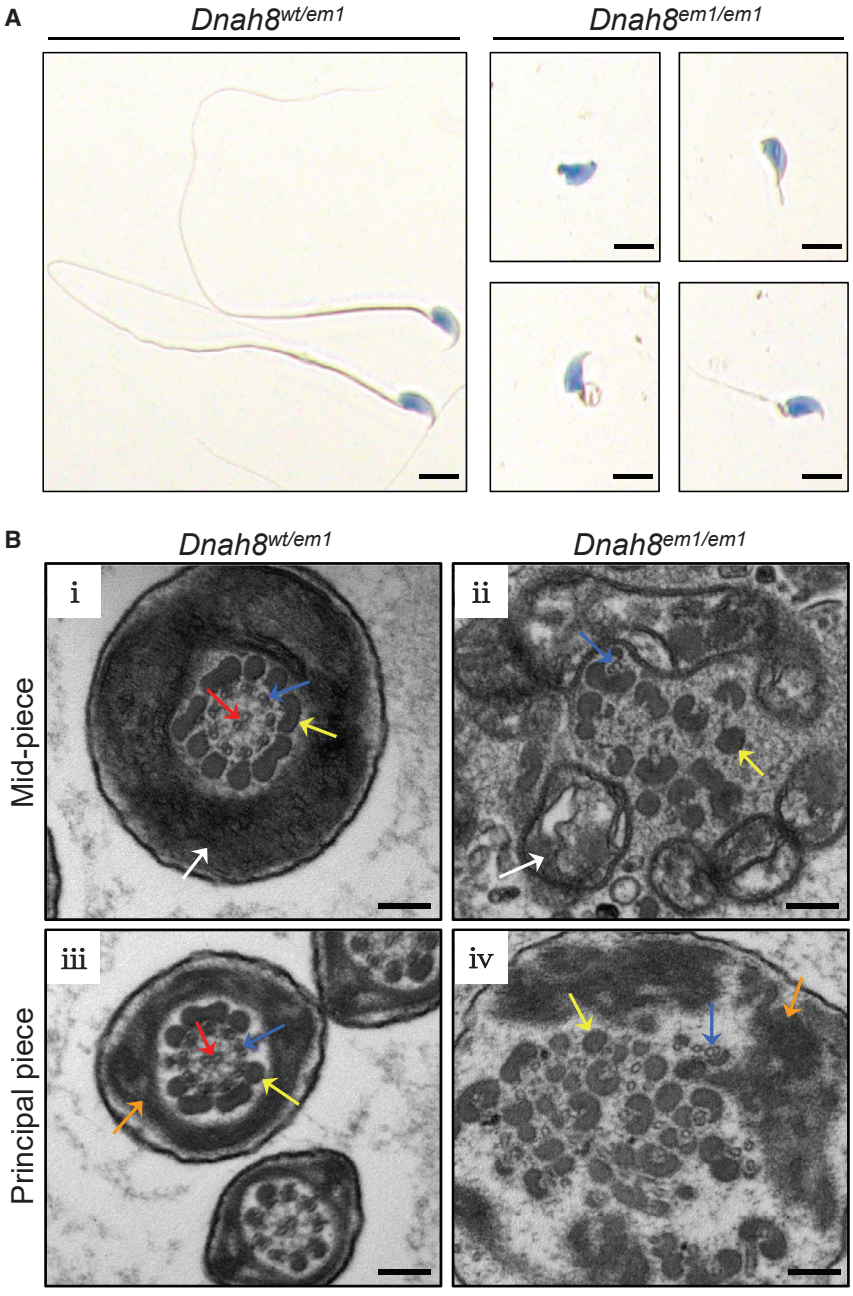

Figure 5. Sperm Morphology and Ultrastructure Analyses for *Dnah8*-KO Male Mice
(A) H&E staining of the spermatozoa obtained from mouse cauda epididymis. The spermatozoa from heterozygous mutated (*Dnah8*$^{wt/em1}$) male mice showed normal morphology. In contrast, *Dnah8*-KO (*Dnah8*$^{em1/em1}$) male mice manifested aberrantflagellar morphologies, which were consistent with the clinical phenotypes in the MMAF-affected men. Scale bar: 5 μm.
(B) TEM of cross-sections of the spermatozoa from *Dnah8*-KO male mice. Cross-sections of the mid-piece (i) and principal piece (iii) of the sperm flagella in heterozygous mutated male mice are shown as controls. (ii) Cross-sections of the mid-piece of the sperm flagella in *Dnah8*-KO male mice revealed disorganization of mitochondrial sheaths, outer dense fibers, and microtubules. (iv) Cross-sections of the principal piece of the sperm flagella in *Dnah8*-KO male mice showed disorganization of fibrous sheaths, outer dense fibers, and microtubules. White arrows indicate mitochondrial sheath, orange arrows indicate fibrous sheaths, yellow arrows indicate outer dense fibers, blue arrows indicate peripheral microtubule doublets, and red arrows indicate the central pair of microtubules. Scale bars: 200 nm.

Further phenotypic analysis revealed that men harboring bi-allelic *DNAH8* variants displayed typical MMAF phenotypes, including reduced sperm motility, missing microtubule doublets, and disassembled or absent ODAs. Intriguingly, ODAs were still present in small amounts on observable doublets in the sperm flagella from subject A051 (who harbored bi-allelic *DNAH8* missense variants), whereas ODAs were absent from those of subject F0300 (who harbored a homozygous frameshift variant of *DNAH8*). This phenomenon may be due to a possible phenotype continuum depending on the severity of variants in MMAF-associated genes, as previously shown for *CFAP70*, *DNAH1*, and *DNAH17*.[2,13,20,33]

Functional experiments further revealed the pathogenicity of bi-allelic *DNAH8* variants. The level of *DNAH8* mRNA in the spermatozoa from subject A051 harboring bi-allelic *DNAH8* missense variants was significantly reduced (Figure S2). This may be due to the recognition of specific sets of mutated mRNAs by RNA-binding proteins, which serve as adaptors and control decay rates by recruitment of RNA-degrading enzymes.[34] The reduced mRNA abundance in low-motility sperm was also previously observed for other members (such as *DNAH1* and *DNAH7*) of the axonemal dynein family.[35]

The remaining mutated mRNA of *DNAH8* may produce a small amount of mis-folded DNAH8 protein. However, the immunostaining of DNAH8 was almost absent in the sperm flagella from men harboring bi-allelic *DNAH8* variants. This near absence of DNAH8 protein may result from specific degradation of unfolded proteins by the "unfolded protein response" described in previous studies.[36,37]

A previous study described the absence of DNAH8 protein in the spermatozoa from men harboring bi-allelic *DNAH17* variants.[13] The present investigations on the amount and localization of DNAH17 revealed a dramatic reduction of DNAH17 in the sperm cells from men harboring bi-allelic *DNAH8* variants. These observations confirm the interaction between DNAH8 and DNAH17 during spermatogenesis. Several previous studies also reported that DNAH8

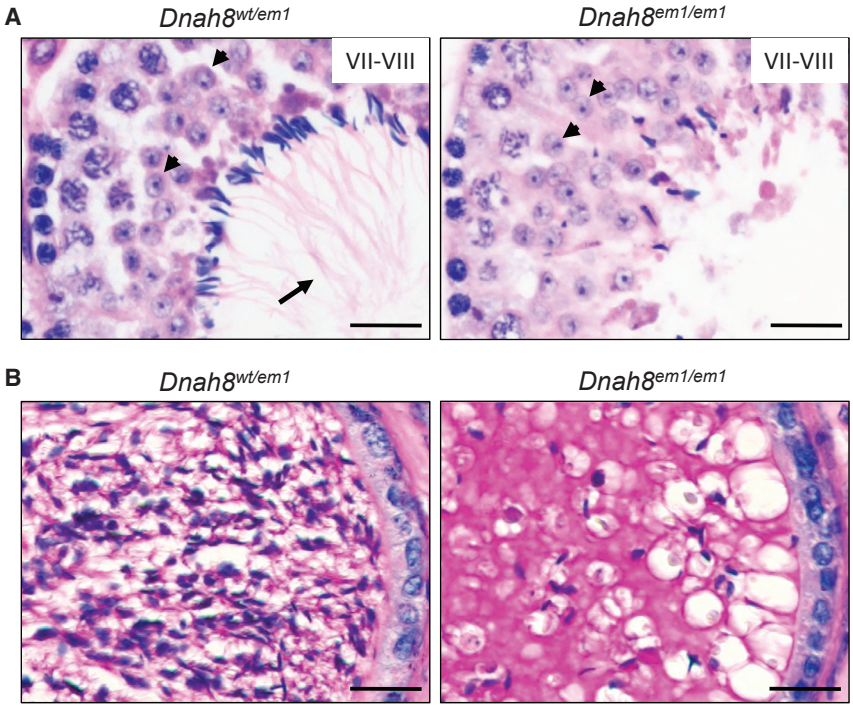

Figure 6. *Dnah8* is Essential for Normal Spermatogenesis in Mice
(A) The development of sperm flagella was investigated in mouse testis through the use of H&E staining. In stage VII–VIII seminiferous tubules, normal round spermatids (arrowheads) were observed, but elongated tails (arrows) were not observed in the testes from *Dnah8*-KO (*Dnah8*$^{em1/em1}$) male mice. Scale bar: 20 μm.
(B) PAS staining of the cauda epididymis from male mice. Decreased sperm quantity was observed in the epididymis from *Dnah8*-KO male mice, when compared with that in heterozygous mutated (*Dnah8*$^{wt/em1}$) male mice. Scale bar: 20 μm.

and DNAH17 were categorically detectable in human sperm proteome analyses.[38,39] DNAH17 is required for flagellar biogenesis and stabilization of microtubule doublets 4–7.[20] Our TEM analysis of sperm also indicated a destabilization of microtubule doublets 4–7 in the principal piece of spermatozoa from men harboring bi-allelic *DNAH8* variants. This characteristic defect shared by DNAH8-associated and DNAH17-associated cases further suggests that DNAH8 and DNAH17 proteins are dependent on each other during flagellar assembly and spermatogenesis.

Presently, *Dnah8*-KO male mice displayed MMAF phenotypes, including diminished sperm motility and abnormal flagella. Furthermore, H&E and PAS staining analyses revealed abnormal spermatogenesis in the testis and reduced sperm counts in the cauda epididymis from *Dnah8*-KO male mice. Previous studies showed that ODAs are preassembled in the cell body and transported as a holo-complex into the cilium, where they dock to the axonemal microtubules via intraflagellar transport (IFT).[40–43] These observations further indicate the important role of ODAs in cell differentiation. Similar results were also found in the spermatozoa with defects in IDA-associated proteins. For example, the spermatozoa from men with *DNAH1* mutations showed severely disarranged axonemal structures with loss of IDAs.[2] All these observations indicate that mutations in dynein proteins not only induce the lack of ODAs and IDAs, but also affect assembly of the axoneme. Therefore, structural abnormalities in the sperm axoneme from men harboring bi-allelic *DNAH8* variants and *Dnah8*-KO male mice are likely caused by the flagellar assembly defects during spermatogenesis. Notably, the decreased sperm counts in *Dnah8*-KO male mice were not observed in men harboring bi-allelic *DNAH8* variants, and this may potentially reflect evolutionarily divergent protein regulatory networks of DNAH8 between human and mouse.

As an assisted reproductive technology, ICSI has been regarded as an effective way to help infertile couples achieve a successful pregnancy. Previous studies have suggested that MMAF-affected men harboring *DNAH1* variants could acquire good prognoses following ICSI, with 70.8% overall fertilization, 50.0% pregnancy, and 37.5% delivery rates.[44] In contrast, ICSI has been reported to fail for the MMAF-affected men carrying *CEP135* (MIM: 611423) or *DNAH17* variants.[13,45] In this study, ICSI experiments were performed using the sperm from *Dnah8*-KO male mice. Although the rate of two-cell embryos in the *Dnah8*-KO group was lower than that of the wild-type control group, we obtained healthy pups, indicating a successful ICSI treatment in the *Dnah8*-KO mouse model. Furthermore, ICSI was also successful for human subject F0300 and resulted in a positive pregnancy outcome and a live birth. Therefore, our findings indicate that ICSI can be recommended for *DNAH8*-associated asthenoteratozoospermia.

In conclusion, we identified *DNAH8* as an asthenoteratozoospermia-associated gene in both humans and mice. The observed effects of DNAH8 deficiency on DNAH17 localization in the sperm flagella further suggested that dynein-arms-associated proteins may affect spermatogenesis in a collaborative manner. Furthermore, *DNAH8*-associated MMAF and male infertility could be treated through the use of ICSI. Our findings will be informative for genetic and reproductive counseling of infertile men with asthenoteratozoospermia.

Data and Code Availability

The NCBI reference sequence number for *DNAH8* transcript is NM_001206927.2. The NCBI reference sequence number for DNAH8 protein is NP_001193856.1.

A

Males providing sperm	No. of oocytes injected	No. of 2-cell embryos	No. of pups delivered
Dnah8$^{wt/wt}$	44	15	2
Dnah8$^{em1/em1}$	81	14	3

B

C

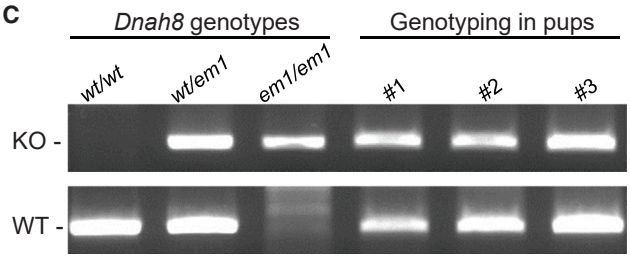

Figure 7. Pups Obtained upon ICSI using the Spermatozoa from *Dnah8*-KO Male Mice

(A) Development of ICSI embryos. Fourteen (17.3%) of the 81 oocytes injected with the spermatozoa from *Dnah8*-KO (*Dnah8*$^{em1/em1}$) male mice developed to the two-cell stage, and three pups were obtained after embryo transfer. ICSI data from the use of sperm from wild-type male mice are shown as controls.
(B) The pups obtained from ICSI using the spermatozoa from *Dnah8*-KO male mice.
(C) Genotyping of these pups. All of the pups carried the heterozygous *Dnah8*-mutated allele. KO denotes the mutated allele and WT denotes the wild-type allele.

Supplemental Data

Supplemental Data can be found online at https://doi.org/10.1016/j.ajhg.2020.06.004.

Acknowledgments

We would like to thank the families for participating and supporting this study. We also thank the Center of Cryo-electron Microscopy at Zhejiang University, the transmission electron microscopy core facility of the Institut Cochin (INSERM U1016, Paris), and Yonggang Lu at Osaka University for technical support. This work was supported by the Ministry of Education, Culture, Sports, Science and Technology (MEXT)/Japan Society for the Promotion of Science (JSPS) (KAKENHI grants JP17H04987 to H.M. and JP19H05750 to M.I.), the National Natural Science Foundation of China (31625015, 31521003, 81901541, 81971441, and 81871200), the Eunice Kennedy Shriver National Institute of Child Health and Human Development (P01HD087157 and R01HD088412 to M.I.), the Bill and Melinda Gates Foundation (INV-001902 to M.I.), the Institut National de la Santé et de la Recherche Médicale (Inserm), the Centre National de la Recherche Scientifique (CNRS), the Université de Paris and the French National Research Agency (MASFLAGELLA ANR-14-CE15-0002 and FLAGEL-OME ANR18-CE17-0014 to P.F.R. and A.T.), Shanghai Medical Center of Key Programs for Female Reproductive Diseases (2017ZZ01016), and Shanghai Municipal Science and Technology Major Project (2017SHZDZX01).

Declaration of Interests

The authors declare no competing interests.

Received: March 19, 2020
Accepted: June 5, 2020
Published: July 2, 2020

Web Resources

1000 Genomes Project, https://www.internationalgenome.org
gnomAD, https://gnomad.broadinstitute.org
HUGO Gene Nomenclature Committee, https://www.genenames.org
Human Protein Atlas, https://www.proteinatlas.org
National Center for Biotechnology Information (NCBI), https://www.ncbi.nlm.nih.gov/
Online Mendelian Inheritance in Man, https://www.omim.org
PolyPhen-2, http://genetics.bwh.harvard.edu/pph2/
SIFT, https://sift.bii.a-star.edu.sg
UniProt, https://www.uniprot.org

References

1. Hosseini, B., Nourmohamadi, M., Hajipour, S., Taghizadeh, M., Asemi, Z., Keshavarz, S.A., and Jafarnejad, S. (2019). The Effect of Omega-3 Fatty Acids, EPA, and/or DHA on Male Infertility: A Systematic Review and Meta-analysis. J. Diet. Suppl. *16*, 245–256.
2. Ben Khelifa, M., Coutton, C., Zouari, R., Karaouzène, T., Rendu, J., Bidart, M., Yassine, S., Pierre, V., Delaroche, J., Hennebicq, S., et al. (2014). Mutations in DNAH1, which encodes an inner arm heavy chain dynein, lead to male infertility from multiple morphological abnormalities of the sperm flagella. Am. J. Hum. Genet. *94*, 95–104.
3. Baccetti, B., Collodel, G., Estenoz, M., Manca, D., Moretti, E., and Piomboni, P. (2005). Gene deletions in an infertile man with sperm fibrous sheath dysplasia. Hum. Reprod. *20*, 2790–2794.
4. Tang, S., Wang, X., Li, W., Yang, X., Li, Z., Liu, W., Li, C., Zhu, Z., Wang, L., Wang, J., et al. (2017). Biallelic Mutations in CFAP43 and CFAP44 Cause Male Infertility with Multiple Morphological Abnormalities of the Sperm Flagella. Am. J. Hum. Genet. *100*, 854–864.
5. Dong, F.N., Amiri-Yekta, A., Martinez, G., Saut, A., Tek, J., Stouvenel, L., Lorès, P., Karaouzène, T., Thierry-Mieg, N., Satre, V., et al. (2018). Absence of CFAP69 Causes Male Infertility due to Multiple Morphological Abnormalities of the Flagella in Human and Mouse. Am. J. Hum. Genet. *102*, 636–648.
6. Kherraf, Z.E., Amiri-Yekta, A., Dacheux, D., Karaouzène, T., Coutton, C., Christou-Kent, M., Martinez, G., Landrein, N., Le Tanno, P., Fourati Ben Mustapha, S., et al. (2018). A Homozygous Ancestral SVA-Insertion-Mediated Deletion in WDR66

Induces Multiple Morphological Abnormalities of the Sperm Flagellum and Male Infertility. Am. J. Hum. Genet. *103*, 400–412.

7. Auguste, Y., Delague, V., Desvignes, J.P., Longepied, G., Gnisci, A., Besnier, P., Levy, N., Beroud, C., Megarbane, A., Metzler-Guillemain, C., and Mitchell, M.J. (2018). Loss of Calmodulin- and Radial-Spoke-Associated Complex Protein CFAP251 Leads to Immotile Spermatozoa Lacking Mitochondria and Infertility in Men. Am. J. Hum. Genet. *103*, 413–420.
8. Coutton, C., Martinez, G., Kherraf, Z.E., Amiri-Yekta, A., Boguenet, M., Saut, A., He, X., Zhang, F., Cristou-Kent, M., Escoffier, J., et al. (2019). Bi-allelic Mutations in ARMC2 Lead to Severe Astheno-Teratozoospermia Due to Sperm Flagellum Malformations in Humans and Mice. Am. J. Hum. Genet. *104*, 331–340.
9. Liu, W., He, X., Yang, S., Zouari, R., Wang, J., Wu, H., Kherraf, Z.E., Liu, C., Coutton, C., Zhao, R., et al. (2019). Bi-allelic Mutations in TTC21A Induce Asthenoteratospermia in Humans and Mice. Am. J. Hum. Genet. *104*, 738–748.
10. Coutton, C., Vargas, A.S., Amiri-Yekta, A., Kherraf, Z.E., Ben Mustapha, S.F., Le Tanno, P., Wambergue-Legrand, C., Karaouzène, T., Martinez, G., Crouzy, S., et al. (2018). Mutations in CFAP43 and CFAP44 cause male infertility and flagellum defects in Trypanosoma and human. Nat. Commun. *9*, 686.
11. Liu, C., He, X., Liu, W., Yang, S., Wang, L., Li, W., Wu, H., Tang, S., Ni, X., Wang, J., et al. (2019). Bi-allelic Mutations in TTC29 Cause Male Subfertility with Asthenoteratospermia in Humans and Mice. Am. J. Hum. Genet. *105*, 1168–1181.
12. Lorès, P., Dacheux, D., Kherraf, Z.E., Nsota Mbango, J.F., Coutton, C., Stouvenel, L., Ialy-Radio, C., Amiri-Yekta, A., Whitfield, M., Schmitt, A., et al. (2019). Mutations in TTC29, Encoding an Evolutionarily Conserved Axonemal Protein, Result in Asthenozoospermia and Male Infertility. Am. J. Hum. Genet. *105*, 1148–1167.
13. Whitfield, M., Thomas, L., Bequignon, E., Schmitt, A., Stouvenel, L., Montantin, G., Tissier, S., Duquesnoy, P., Copin, B., Chantot, S., et al. (2019). Mutations in DNAH17, Encoding a Sperm-Specific Axonemal Outer Dynein Arm Heavy Chain, Cause Isolated Male Infertility Due to Asthenozoospermia. Am. J. Hum. Genet. *105*, 198–212.
14. Touré, A., Martinez, G., Kherraf, Z.E., Cazin, C., Beurois, J., Arnoult, C., Ray, P.F., and Coutton, C. (2020). The genetic architecture of morphological abnormalities of the sperm tail. Hum. Genet. https://doi.org/10.1007/s00439-00020-02113-x.
15. Reiter, J.F., and Leroux, M.R. (2017). Genes and molecular pathways underpinning ciliopathies. Nat. Rev. Mol. Cell Biol. *18*, 533–547.
16. Zariwala, M.A., Knowles, M.R., and Omran, H. (2007). Genetic defects in ciliary structure and function. Annu. Rev. Physiol. *69*, 423–450.
17. Ishikawa, T. (2017). Axoneme Structure from Motile Cilia. Cold Spring Harb. Perspect. Biol. *9*, a028076.
18. Loges, N.T., Olbrich, H., Fenske, L., Mussaffi, H., Horvath, J., Fliegauf, M., Kuhl, H., Baktai, G., Peterffy, E., Chodhari, R., et al. (2008). DNAI2 mutations cause primary ciliary dyskinesia with defects in the outer dynein arm. Am. J. Hum. Genet. *83*, 547–558.
19. Ibañez-Tallon, I., Heintz, N., and Omran, H. (2003). To beat or not to beat: roles of cilia in development and disease. Hum. Mol. Genet. *12*, R27–R35.
20. Zhang, B., Ma, H., Khan, T., Ma, A., Li, T., Zhang, H., Gao, J., Zhou, J., Li, Y., Yu, C., et al. (2020). A DNAH17 missense variant causes flagella destabilization and asthenozoospermia. J. Exp. Med. *217*, e20182365.
21. Wang, Y., Yang, J., Jia, Y., Xiong, C., Meng, T., Guan, H., Xia, W., Ding, M., and Yuchi, M. (2014). Variability in the morphologic assessment of human sperm: use of the strict criteria recommended by the World Health Organization in 2010. Fertil. Steril. *101*, 945–949.
22. Samant, S.A., Ogunkua, O.O., Hui, L., Lu, J., Han, Y., Orth, J.M., and Pilder, S.H. (2005). The mouse t complex distorter/sterility candidate, Dnahc8, expresses a gamma-type axonemal dynein heavy chain isoform confined to the principal piece of the sperm tail. Dev. Biol. *285*, 57–69.
23. Chemes, H.E., and Alvarez Sedo, C. (2012). Tales of the tail and sperm head aches: changing concepts on the prognostic significance of sperm pathologies affecting the head, neck and tail. Asian J. Androl. *14*, 14–23.
24. Viswanadha, R., Sale, W.S., and Porter, M.E. (2017). Ciliary Motility: Regulation of Axonemal Dynein Motors. Cold Spring Harb. Perspect. Biol. *9*, a018325.
25. Loges, N.T., Antony, D., Maver, A., Deardorff, M.A., Güleç, E.Y., Gezdirici, A., Nöthe-Menchen, T., Höben, I.M., Jelten, L., Frank, D., et al. (2018). Recessive DNAH9 Loss-of-Function Mutations Cause Laterality Defects and Subtle Respiratory Ciliary-Beating Defects. Am. J. Hum. Genet. *103*, 995–1008.
26. King, S.M. (2016). Axonemal Dynein Arms. Cold Spring Harb. Perspect. Biol. *8*, a028100.
27. Pazour, G.J., Agrin, N., Walker, B.L., and Witman, G.B. (2006). Identification of predicted human outer dynein arm genes: candidates for primary ciliary dyskinesia genes. J. Med. Genet. *43*, 62–73.
28. Fliegauf, M., Olbrich, H., Horvath, J., Wildhaber, J.H., Zariwala, M.A., Kennedy, M., Knowles, M.R., and Omran, H. (2005). Mislocalization of DNAH5 and DNAH9 in respiratory cells from patients with primary ciliary dyskinesia. Am. J. Respir. Crit. Care Med. *171*, 1343–1349.
29. Dougherty, G.W., Loges, N.T., Klinkenbusch, J.A., Olbrich, H., Pennekamp, P., Menchen, T., Raidt, J., Wallmeier, J., Werner, C., Westermann, C., et al. (2016). DNAH11 Localization in the Proximal Region of Respiratory Cilia Defines Distinct Outer Dynein Arm Complexes. Am. J. Respir. Cell Mol. Biol. *55*, 213–224.
30. Liu, S., Chen, W., Zhan, Y., Li, S., Ma, X., Ma, D., Sheng, W., and Huang, G. (2019). DNAH11 variants and its association with congenital heart disease and heterotaxy syndrome. Sci. Rep. *9*, 6683.
31. Guichard, C., Harricane, M.C., Lafitte, J.J., Godard, P., Zaegel, M., Tack, V., Lalau, G., and Bouvagnet, P. (2001). Axonemal dynein intermediate-chain gene (DNAI1) mutations result in situs inversus and primary ciliary dyskinesia (Kartagener syndrome). Am. J. Hum. Genet. *68*, 1030–1035.
32. Fassad, M.R., Shoemark, A., Legendre, M., Hirst, R.A., Koll, F., le Borgne, P., Louis, B., Daudvohra, F., Patel, M.P., Thomas, L., et al. (2018). Mutations in Outer Dynein Arm Heavy Chain DNAH9 Cause Motile Cilia Defects and Situs Inversus. Am. J. Hum. Genet. *103*, 984–994.
33. Beurois, J., Martinez, G., Cazin, C., Kherraf, Z.E., Amiri-Yekta, A., Thierry-Mieg, N., Bidart, M., Petre, G., Satre, V., Brouillet, S., et al. (2019). CFAP70 mutations lead to male infertility due to severe astheno-teratozoospermia. A case report. Hum. Reprod. *34*, 2071–2079.

34. Stoecklin, G., and Mühlemann, O. (2013). RNA decay mechanisms: specificity through diversity. Biochim. Biophys. Acta *1829*, 487–490.
35. Caballero-Campo, P., Lira-Albarrán, S., Barrera, D., Borja-Cacho, E., Godoy-Morales, H.S., Rangel-Escareño, C., Larrea, F., and Chirinos, M. (2020). Gene transcription profiling of astheno- and normo-zoospermic sperm subpopulations. Asian J. Androl. *22*. https://doi.org/10.4103/aja.aja_4143_4119.
36. Rutkowski, D.T., and Hegde, R.S. (2010). Regulation of basal cellular physiology by the homeostatic unfolded protein response. J. Cell Biol. *189*, 783–794.
37. Wang, S., and Kaufman, R.J. (2012). The impact of the unfolded protein response on human disease. J. Cell Biol. *197*, 857–867.
38. Wang, G., Guo, Y., Zhou, T., Shi, X., Yu, J., Yang, Y., Wu, Y., Wang, J., Liu, M., Chen, X., et al. (2013). In-depth proteomic analysis of the human sperm reveals complex protein compositions. J. Proteomics *79*, 114–122.
39. Amaral, A., Castillo, J., Estanyol, J.M., Ballescà, J.L., Ramalho-Santos, J., and Oliva, R. (2013). Human sperm tail proteome suggests new endogenous metabolic pathways. Mol. Cell. Proteomics *12*, 330–342.
40. Fowkes, M.E., and Mitchell, D.R. (1998). The role of preassembled cytoplasmic complexes in assembly of flagellar dynein subunits. Mol. Biol. Cell *9*, 2337–2347.
41. Dean, A.B., and Mitchell, D.R. (2013). Chlamydomonas ODA10 is a conserved axonemal protein that plays a unique role in outer dynein arm assembly. Mol. Biol. Cell *24*, 3689–3696.
42. Dean, A.B., and Mitchell, D.R. (2015). Late steps in cytoplasmic maturation of assembly-competent axonemal outer arm dynein in Chlamydomonas require interaction of ODA5 and ODA10 in a complex. Mol. Biol. Cell *26*, 3596–3605.
43. Desai, P.B., Freshour, J.R., and Mitchell, D.R. (2015). Chlamydomonas axonemal dynein assembly locus ODA8 encodes a conserved flagellar protein needed for cytoplasmic maturation of outer dynein arm complexes. Cytoskeleton (Hoboken) *72*, 16–28.
44. Wambergue, C., Zouari, R., Fourati Ben Mustapha, S., Martinez, G., Devillard, F., Hennebicq, S., Satre, V., Brouillet, S., Halouani, L., Marrakchi, O., et al. (2016). Patients with multiple morphological abnormalities of the sperm flagella due to DNAH1 mutations have a good prognosis following intracytoplasmic sperm injection. Hum. Reprod. *31*, 1164–1172.
45. Sha, Y.W., Xu, X., Mei, L.B., Li, P., Su, Z.Y., He, X.Q., and Li, L. (2017). A homozygous CEP135 mutation is associated with multiple morphological abnormalities of the sperm flagella (MMAF). Gene *633*, 48–53.
46. Cooper, T.G., Noonan, E., von Eckardstein, S., Auger, J., Baker, H.W., Behre, H.M., Haugen, T.B., Kruger, T., Wang, C., Mbizvo, M.T., and Vogelsong, K.M. (2010). World Health Organization reference values for human semen characteristics. Hum. Reprod. Update *16*, 231–245.
47. Auger, J., Jouannet, P., and Eustache, F. (2016). Another look at human sperm morphology. Hum. Reprod. *31*, 10–23.

The American Journal of Human Genetics, Volume *107*

Supplemental Data

Bi-allelic *DNAH8* Variants Lead to Multiple Morphological Abnormalities of the Sperm Flagella and Primary Male Infertility

Chunyu Liu, Haruhiko Miyata, Yang Gao, Yanwei Sha, Shuyan Tang, Zoulan Xu, Marjorie Whitfield, Catherine Patrat, Huan Wu, Emmanuel Dulioust, Shixiong Tian, Keisuke Shimada, Jiangshan Cong, Taichi Noda, Hang Li, Akane Morohoshi, Caroline Cazin, Zine-Eddine Kherraf, Christophe Arnoult, Li Jin, Xiaojin He, Pierre F. Ray, Yunxia Cao, Aminata Touré, Feng Zhang, and Masahito Ikawa

Supplemental Note: Case Reports

All the cases of this study were examined carefully to exclude primary ciliary dyskinesia associated symptoms such as sinusitis, bronchitis, pneumonia and otitis media.[1] These men had normal development of male external genitalia, bilateral testicular sizes, hormone levels, and secondary sexual characteristics. Chromosomal karyotypes of these subjects were also normal, and no microdeletions were found in the human Y chromosome. Furthermore, three healthy men with normal fertility served as control subjects. Informed consents were obtained from all subjects participating in the study. This study was approved by the institutional review boards at all the participating institutes.

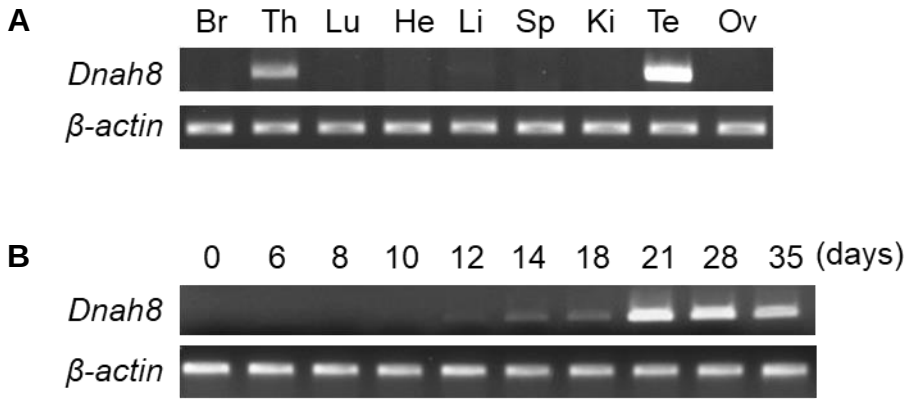

Figure S1. Expressions of Mouse *Dnah8* in Different Tissues and Postnatal Testes.

(A) Expressions of *Dnah8* were investigated by RT-PCR in various tissues from adult male mice. *β-actin* was used as an internal control locus. Br, brain; Th, thymus; Lu, lung; He, heart; Li, liver; Sp, spleen; Ki, kidney; Te, testis; Ov, ovary. (B) Expressions of mouse *Dnah8* were analyzed by RT-PCR using testicular tissues from male mice of different days after birth.

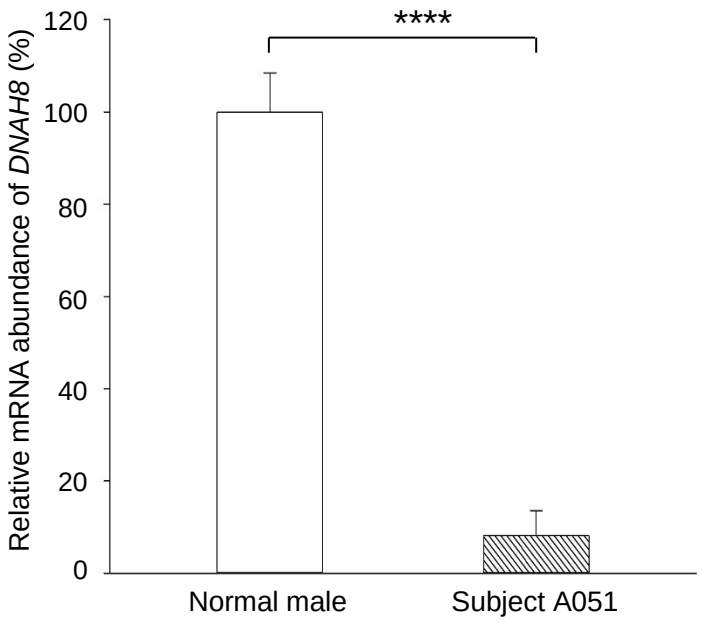

Figure S2. Measure of *DNAH8* mRNA Abundance in the Spermatozoa from a Normal Male Control and Subject A051 Harboring Bi-allelic *DNAH8* Variants.

RT-qPCR assays suggested that the level of *DNAH8* mRNA was dramatically reduced in the sperm from subject A051 when compared to that of a normal male control. The experiments were performed three times and statistical analysis was performed using two-tailed Student's paired or unpaired *t* tests. Data represent the means ± standard error of the means (S.E.M.). **** $P < 0.0001$.

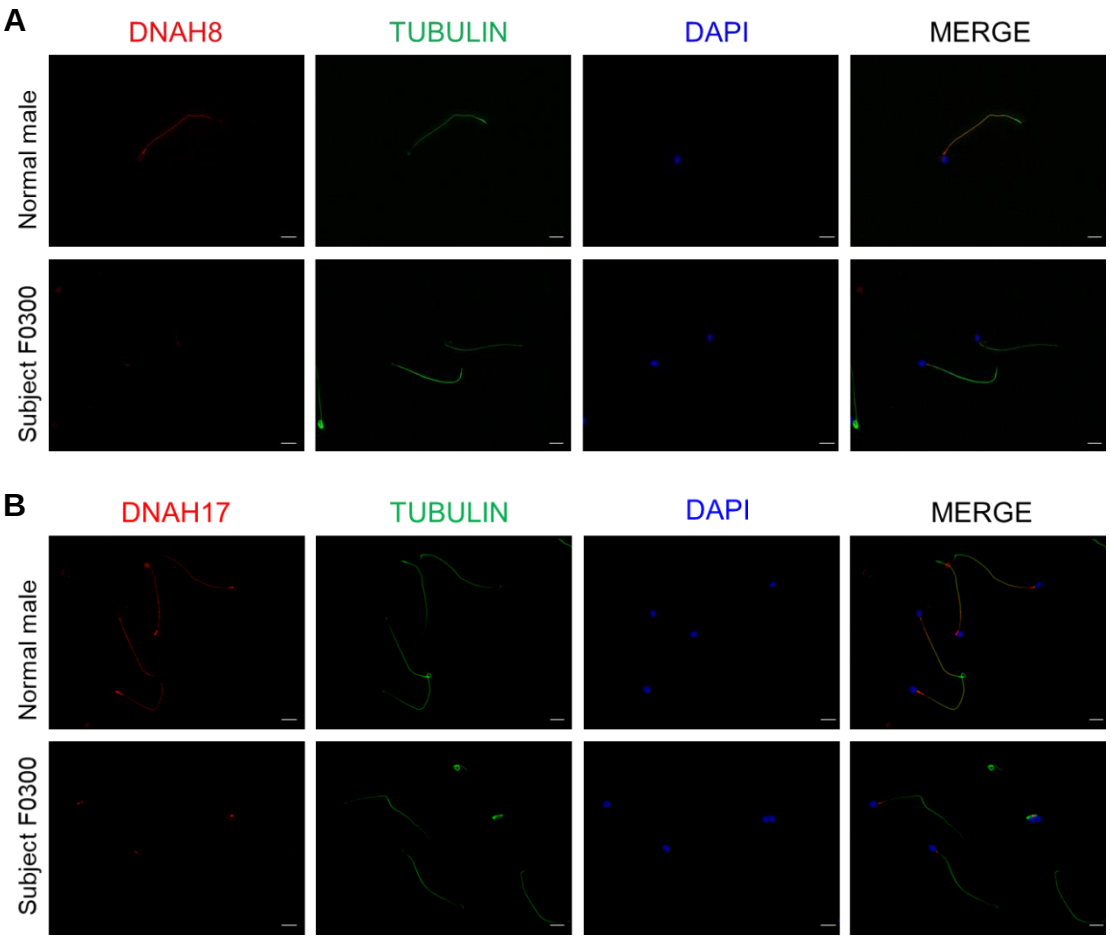

Figure S3. Immunostaining of DNAH8 and DNAH17 in the Spermatozoa from a Normal Male Control and Subject F0300 Harboring a Homozygous *DNAH8* Frameshift Variant.

(A) Immunofluorescence staining of the spermatozoa from a control and subject F0300 with anti-DNAH8 (red) and anti-α-tubulin (green) antibodies. (B) Immunofluorescence of the spermatozoa from a control and subject F0300 with anti-DNAH17 (red) and anti-α-tubulin (green) antibodies. Spermatozoa were counterstained with DAPI (blue) as a nuclei marker. The scale bars represent 5 μm.

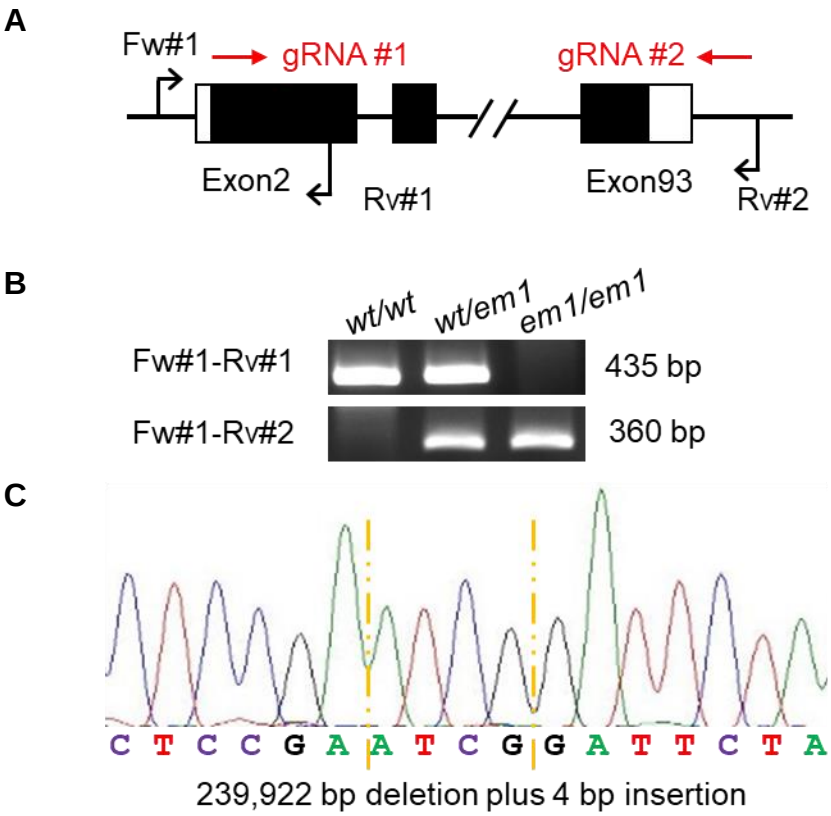

Figure S4. CRISPR/Cas9 Targeting Scheme for Generating *Dnah8*-KO (*em1/em1*) Mice.

(A) The gRNAs were targeted in exons 2 and 93 of mouse *Dnah8* to delete the entire coding region. (B) Mouse genotyping with specific primers. Primers Fw#1 and Rv#1 were used for the wild-type allele (*wt*), and primers Fw#1 and Rv#2 were used for the *Dnah8* mutated allele (*em1*). (C) Sanger sequencing result of *Dnah8*$^{em1/em1}$ mice showed a 239922-bp deletion plus a 4-bp insertion.

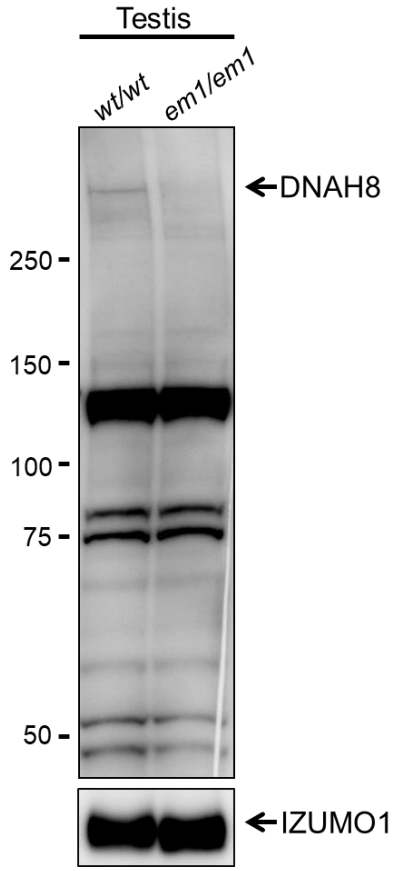

Figure S5. Expression Analysis of DNAH8 Protein in the Testes from Wild-type (*wt/wt*) and *Dnah8*-KO (*em1/em1*) Male Mice.

Western blotting analysis revealed the almost absence of DNAH8 protein in the spermatozoa from *Dnah8*-KO male mice. IZUMO1 was used as a loading control.

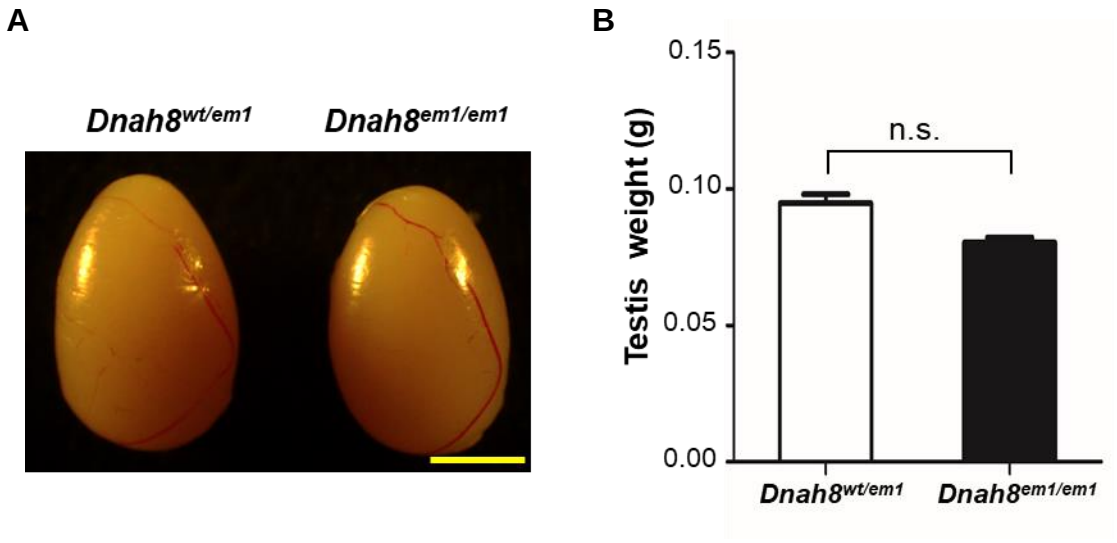

Figure S6. Testis Sizes and Weights in *Dnah8*-KO (*Dnah8*$^{em1/em1}$) Male Mice and Heterozygous Mutated (*Dnah8*$^{wt/em1}$) Male Mice.

(A) Testis Sizes of the Mouse Model. The scale bar represents 2 mm. (B) No significant difference was observed in testis weights between *Dnah8*$^{em1/em1}$ and *Dnah8*$^{wt/em1}$ male mice. Data represent the means ± SEM; n.s., not significant.

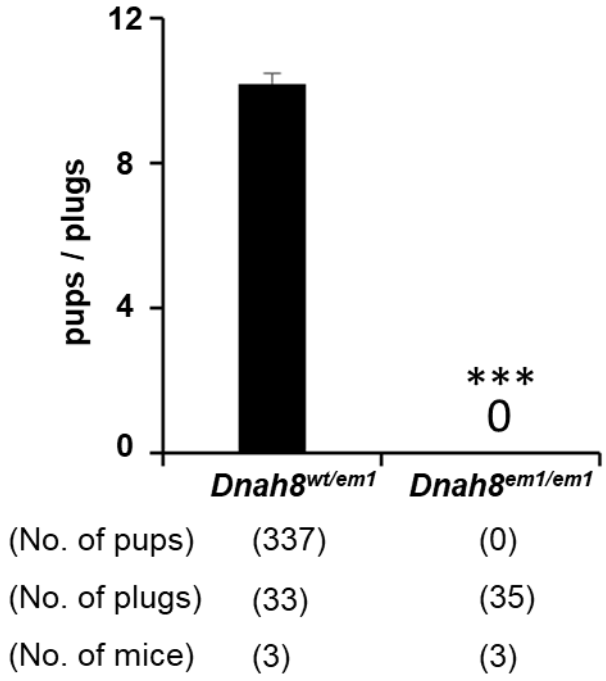

Figure S7. Fertility of *Dnah8*-KO (*Dnah8*$^{em1/em1}$) Male Mice and Heterozygous Mutated (*Dnah8*$^{wt/em1}$) Male Mice.

Dnah8$^{wt/em1}$ (3 males) and *Dnah8*$^{em1/em1}$ (3 males) mice were examined in this assay. Each male mouse was bred with three wild-type female mice, and the plugs & pups were measured. *Dnah8*$^{em1/em1}$ males were sterile. Unpaired *t* test: ***$P < 0.001$; the error bar represents the standard deviation.

Table S1. Primers Used for Verification of Human *DNAH8* Variants.

Primer Name	Primer Sequence (5'-3')	Tm
M1-F	TAGTCTGTCAGCAGGAATG	61 ℃
M1-R	AAAGAGTAGAAATACAAGCA	
M2-F	ACTGTTGCTATGATGGTTC	49 ℃
M2-R	ACTATTGCTAGGAGGAAAG	
M3-F	TGGACTTTGGCAGTGAATTG	58 ℃
M3-R	GTGGAGCTGGACGAGGTTAC	
M4-F	TTGCCCCCACTTTATGTACC	61 ℃
M4-R	ACCACTGGCCATCTCCTAAA	
M5-F	GCACATCCCAGCTAGCTGAT	60 ℃
M5-R	AGACATCTGCGTTGTTCCGT	

Table S2. Rates of Ultrastructural Abnormalities in the Spermatozoa from Men Carrying Bi-allelic *DNAH8* Variants.

	Control[a] (n=50)	Subject A051 (n=40)	Subject X003 (n=40)	Subject F0300 (n=34)
Missing CP	1 (2.0%)	11 (27.5%)	16 (40.0%)	3 (8.8%)
Missing MT	6 (12.0%)	15 (37.5%)	10 (25.0%)	5 (14.7%)
Global disorganization	1 (2.0%)	11 (27.5%)	12 (30.0%)	13 (38.2%)
Normal sections	42 (84.0%)	3 (7.5%)	2 (5.0%)	13 (38.2%)

[a]Values represent the mean of three normal males; n, number of cross sections for analysis.

Abbreviations: CP, central pair of microtubules; MT, peripheral microtubule doublet.

Table S3. Primers Used for RT-qPCR Analysis.

Primer Name	Primer Sequence (5'-3')	Tm
H-*DNAH8*-F	CAGCAGCTGAGGTAAGTGAA	60 ℃
H-*DNAH8*-R	CTCTTTTGAGGTAGTGGTGA	
H-*GAPDH*-F	GGAGCGAGATCCCTCCAAAAT	60 ℃
H-*GAPDH*-R	GGCTGTTGTCATACTTCTCATGG	

Table S4. Primers Used for RT-PCR Analysis.

Primer Name	Primer Sequence (5'-3')	Tm
M-*Dnah8*-F	CAGGTCCACTATGACTTTGG	65 ℃
M-*Dnah8*-R	AGATCCCATCTGTCCAGTCG	
M-*β-actin*-F	CATCCGTAAAGACCTCTATGCCAAC	65 ℃
M-*β-actin*-R	ATGGAGCCACCGATCCACA	

Supplemental Material and Methods

Whole-Exome Sequencing (WES) and Bioinformatic Analysis

WES was performed on the 90 Chinese MMAF-affected men according to our previously described protocol.[2,3] Briefly, genomic DNAs were isolated from peripheral blood samples of human subjects using the DNeasy Blood and Tissue Kit (QIAGEN, Germany). The human exome was enriched by SureSelect XT Human All Exon Kit (Agilent, USA), and then sequenced with the Illumina HiSeq X-TEN platform at Cloud Health Genomics (Shanghai, China). The obtained data were mapped to the human genome assembly hg19 by the Burrows-Wheeler Aligner (BWA) software. The Picard software was employed to remove PCR duplicates and evaluate the quality of variants by attaining effective reads, effective base, average coverage depth, and 90× – 120× coverage ratio.[4] For the 167 MMAF-affected men in the second cohort, WES and bioinformatic analyses were performed with a previously described protocol using the human genome assembly GRCh38.[5] The ANNOVAR software was used for functional annotation with OMIM, Gene Ontology, KEGG Pathway, SIFT, PolyPhen-2, MutationTaster, 1000 Genomes Project, and the gnomAD database.[6-11] Sanger sequencing was employed for variant validation using the primers listed in Table S1.

Animals

All animal experiments were approved by the Animal Care and Use Committee of the Research Institute for Microbial Diseases, Osaka University. Mice were purchased from Japan SLC or CLEA Japan.

Y Chromosome Microdeletion Analysis

The analysis of Y chromosome microdeletion was performed using the Y Chromosome Microdeletions Detection Kit (Tellgen, Shanghai, China) according to the manufacturer's

protocol as described in previous study.[12] Briefly, genomic DNA was extracted from peripheral blood lymphocytes and multiplex polymerase chain reaction (PCR) was performed to detect the deletions of following sequence-tagged sites: AZFa, sY84 and sY86; AZFb, sY127 and sY134; and AZFc, sY254 and sY255. *ZFX/ZFY* and *SRY* were used as internal control loci, and positive control DNA samples were obtained from men with normal spermatogenesis.

Semen Characteristics Analysis

Semen sample of men harboring bi-allelic *DNAH8* variants were obtained by masturbation after a period of 3 to 7 days of sexual abstinence and examined after liquefaction for 30 min at 37℃. Semen volume, sperm concentration and motility were evaluated by the Sperm Class Analyzer CASA System (Spain) in the source hospitals during routine examination. Morphological analysis of the sperm cells was performed with hematoxylin and eosin (H&E) staining and scanning electron microscopy (SEM). Morphological abnormalities of the sperm flagella were classified into five categories as absent, short, bent, coiled flagella and flagella of irregular caliber according to World Health Organization guidelines.[13] For each subject, at least 200 spermatozoa were counted to evaluate the percentages of morphologically abnormal spermatozoa.

To examine sperm morphology and motility of mice, spermatozoa were extracted from the cauda epididymes, and then dispersed in TYH medium for 10 min.[14] Sperm morphology and motility were observed under an Olympus BX53 differential interference contrast microscopy equipped with an Olympus DP74 color camera (Olympus, Japan).

Real-time Quantitative PCR (RT-qPCR) and Reverse Transcription PCR (RT-PCR)

For RT-qPCR**,** total RNAs were extracted from human spermatozoa using the Allprep DNA/RNA/Protein Mini Kit (QIAGEN). Approximately 0.5 ug of obtained RNAs were

converted into cDNAs with Hiscript ll Q RT SuperMix for qPCR (Vazyme). Then the RT-qPCR was performed using AceQ qPCR SYBR Green Master Mix (Vazyme) on a CFX Connect™ Real–Time PCR Detection System. Each assay was performed in triplicate for each sample, and the human *GAPDH* gene was used as an internal control locus. The $2^{-\Delta\Delta Ct}$ method was used for data analysis. The primers for RT-qPCR are listed in Table S3.

For RT-PCR**,** total RNAs were extracted from various tissues of adult C57BL/6N mice or testes from 1- to 5-week-old C57BL/6N males, and then converted to cDNA with SuperScript III First Strand Synthesis System (Thermo Fisher) using an oligo (dT) primer. PCR was performed using 10 ng of cDNA, and the primers were listed in Table S4. The amplification conditions were 3 min at 94 ℃, followed by 35 cycles of 94 ℃ for 30 s, 65 ℃ for 30 s, and 72 ℃ for 30 s, with a final two-minute extension at 72 ℃.

Immunofluorescence Analysis

Immunofluorescence (IF) experiments were conducted using the sperm cells from case and control subjects. After washes in phosphate-buffered saline (PBS), the sperm cells were fixed in 4% paraformaldehyde for 30 min at room temperature and coated on the slides treated with 0.1% poly L-lysine pre-coated slides (Thermo Fisher). Then the slides were blocked in 10% donkey serum for 1h and incubated overnight at 4 ℃ with the following primary antibodies: rabbit polyclonal anti-DNAH8 (bs-14367R, Bioss, 1:100 and HPA 028447, Sigma, 1/2000), rabbit polyclonal anti-DNAH17 (24488-1-AP, Proteintech, 1:100 and HPA 024354, Sigma, 1:200), and monoclonal mouse anti-α-tubulin (T9026, Sigma, 1:500). Next, washes were performed using PBS with 0.1% (v/v) Tween20, followed by an hour incubation at room temperature with highly cross-absorbed secondary antibodies Alexa Fluor 488 anti-Mouse IgG (1:1000, 34106ES60, Yeasen) and Cy3-conjugated AffiniPure Goat Anti-Rabbit IgG (1:4000, 111-165-003, Jackson). Fluorescence images were captured with a confocal microscope

(Zeiss LSM 880).

Electron Microscopy Analysis

For SEM assay, the sperm samples were fixed in 2.5% glutaraldehyde, rinsed in 0.1 mol/L phosphate buffer for 30 min, and post-fixed in osmic acid. Next, the specimens were rinsed thoroughly again in 0.1 mol/L phosphate buffer for 30 min, progressively dehydrated with an ethanol and isoamyl acetate gradient, and dried by a CO_2 critical-point dryer (Eiko HCP-2, Hitachi). Afterward, the specimens were mounted on aluminum stubs, sputter coated by an ionic sprayer meter (Eiko E-1020, Hitachi), and analyzed by SEM (Stereoscan 260) under an accelerating voltage of 20 kV.

Transmission electron microscopy (TEM) assay for human sperm samples was performed according to a previously described protocol.[15] Briefly, semen samples were rinsed and fixed in glutaraldehyde. Dehydration was performed using graded ethanol (50%, 70%, 90%, and 100%) and 100% acetone followed by infiltration with 1:1 acetone and SPI-Chem resin overnight at 37 ℃. After infiltration and being embedded in Epon 812, ultrathin sections were stained with uranyl acetate and lead citrate, and then observed and photographed by TEM (TECNAI-10, Philips) with an accelerating voltage of 80 kV.

For TEM analysis of mouse sperm, cauda epididymis samples were prepared as described previously.[16] The sections were observed using a JEM-1400 plus electron microscope (JEOL, Japan) at 80 kV with a CCD Veleta 2K×2K camera (Olympus).

Generation of *Dnah8*-knockout (*Dnah8*-KO) Mice by CRISPR-Cas9

The *Dnah8*-KO mouse model was generated using the CRISPR-Cas9 technology based on the B6D2F1 mouse strains. The guide RNAs were designed against the regions near the start codon (gRNA #1: 5′-GCCACCCCCTCCGAGTGAAG-3′) and stop codon (gRNA #2: 5′-TAGAATCAGAAGCGTGAATT-3′) to delete the entire coding region. To

check gRNAs/Cas9 cleavage efficiency, plasmids expressing hCas9 and gRNAs were prepared by ligating oligonucleotides into the *Bbs*I site of pX459.[17] The pCAG-EGxxFP reporter plasmids were prepared as previously described[18] using 5′-AGTTGAGATCCCCTCTACCC-3′ (plus *Nhe*I site) (Fw #1) and 5′-GTCAGTCACGGAAGTAGCAGG-3′ (plus *Sal*I site) (Rv #1) to clone the genomic region near the start codon and primers 5′-CCTCACCTTCATCACCGTGG-3′ (plus *Nhe*I site) and 5′-CTGGGGTCCTTTTAGGAGGG-3′ (plus *Sal*I site) (Rv #2) to clone the genomic region near the stop codon. Confirmation of gRNAs/Cas9 cleavage efficiency was performed by transfecting HEK293T cells with pCAG-EGxxFP and pX459 plasmids, as previously reported.[18]

For generating KO mice, superovulation-induced B6D2F1 female mice were mated with B6D2F1 males, and fertilized eggs were collected from the oviduct. Two-pronuclear zygotes were electroporated with crRNA/tracrRNA/Cas9 ribonucleoprotein complexes using a NEPA21 Super Electroporator (NEPAGENE, Japan).[19] The treated zygotes were cultured in KSOM medium[20] to the two-cell stage and transplanted into the oviducts of pseudopregnant ICR females at 0.5 day after mating with vasectomized males. The *Dnah8*-mutated F0 mice carrying large deletions were identified by genomic PCR using the same primer sets as those used for the construction of pCAG-EGxxFP (Fw#1 and Rv#1 for the WT allele, Fw#1 and Rv#2 for the KO allele). The DNA sequence of the mutant alleles was further confirmed by Sanger sequencing. After genotype validation, *Dnah8* mutated F0 mice underwent serial mating to generate homozygous offspring.

Western Blotting Analysis

Whole protein extracts from mouse testes were obtained in lysis buffer (6M urea, 2M thiourea, 2% sodium deoxycholate). The protein samples were separated by sodium dodecyl sulfate polyacrylamide gel electrophoresis (SDS-PAGE) and transferred onto polyvinylidene difluoride membrane (Immobilon-P, Merck Millipore, USA). Then the

membranes were blocked with 10% skimmed milk (Nacalai tesque, Japan) and incubated with rabbit anti-DNAH8 (#ab121989, Abcam, UK) or rat anti-IZUMO1 (#KS64-125)[21] antibodies overnight at 4℃, followed by horseradish peroxidase (HRP)-conjugated secondary antibodies (#111-036-045 or #112-035-167, Jackson ImmunoResearch, USA) for 2 hours at room temperature. Detection was carried out with Chemi-Lumi One Super (Nacalai tesque).

Periodic Acid-Schiff (PAS) Staining

Epididymal tissue samples from male mice were fixed in Bouin's solution (Polysciences, USA) and further processed for paraffin embedding. Paraffin sections were cut at a thickness of 5-μm on a Microm HM325 microtome (Microm, Germany), stained with 1% periodic acid (Nacalai Tesque) and Schiff's reagent (Wako, Japan), followed by counterstaining with Mayer hematoxylin solution (FUJIFILM WakoPure Chemical, Japan).

H&E Staining

Fresh testicular tissue samples from male mice were fixed in Bouin's solution (Polysciences) and embedded in paraffin. Sections were cut at a 5-μm thickness on a Microm HM325 microtome (Microm) and stained with Mayer hematoxylin solution and 1% eosin Y solution (FUJIFILM WakoPure Chemical). For staining mouse spermatozoa, samples were collected from cauda epididymes, washed in PBS, fixed in 4% PFA and stained in the same way as the testes.

Intracytoplasmic Sperm Injection (ICSI)

B6D2F1 female mice were superovulated by injecting equine chorionic gonadotropin (eCG, ASKA Animal Health, Japan) and human chorionic gonadotropin (hCG, ASKA Animal Health) with 48 hours interval. Mature oocytes were collected 14 hours after the

hCG injection. After treatment with 1 mg/mL of hyaluronidase (FUJIFILM Wako Pure Chemical) for 5 min to remove the cumulus cells, oocytes were placed in KSOM medium at 37℃ under 5% CO_2 in air until subjected to ICSI. For wild-type male mice, sperm heads were separated from the tails by applying a few piezo pulses. For *Dnah8*-KO male mice, the whole sperm was used for ICSI due to the difficulty for separating the head and tail. The sperm head or the whole sperm was injected into a mature oocyte using a piezo manipulator (PrimeTech, Japan). Then, 2-cell embryos were transferred to pseudopregnant ICR females on the next day.

Supplemental References

1. Knowles, M.R., Zariwala, M., and Leigh, M. (2016). Primary Ciliary Dyskinesia. Clin Chest Med *37*, 449-461.
2. Tang, S., Wang, X., Li, W., Yang, X., Li, Z., Liu, W., Li, C., Zhu, Z., Wang, L., Wang, J., et al. (2017). Biallelic Mutations in CFAP43 and CFAP44 Cause Male Infertility with Multiple Morphological Abnormalities of the Sperm Flagella. Am J Hum Genet *100*, 854-864.
3. Liu, W., He, X., Yang, S., Zouari, R., Wang, J., Wu, H., Kherraf, Z.E., Liu, C., Coutton, C., Zhao, R., et al. (2019). Bi-allelic Mutations in TTC21A Induce Asthenoteratospermia in Humans and Mice. Am J Hum Genet *104*, 738-748.
4. Li, H., and Durbin, R. (2010). Fast and accurate long-read alignment with Burrows-Wheeler transform. Bioinformatics *26*, 589-595.
5. Coutton, C., Martinez, G., Kherraf, Z.E., Amiri-Yekta, A., Boguenet, M., Saut, A., He, X., Zhang, F., Cristou-Kent, M., Escoffier, J., et al. (2019). Bi-allelic Mutations in ARMC2 Lead to Severe Astheno-Teratozoospermia Due to Sperm Flagellum Malformations in Humans and Mice. Am J Hum Genet *104*, 331-340.
6. Wang, K., Li, M., and Hakonarson, H. (2010). ANNOVAR: functional annotation of genetic variants from high-throughput sequencing data. Nucleic Acids Res *38*, e164.
7. Ashburner, M., Ball, C.A., Blake, J.A., Botstein, D., Butler, H., Cherry, J.M., Davis, A.P., Dolinski, K., Dwight, S.S., Eppig, J.T., et al. (2000). Gene ontology: tool for the unification of biology. The Gene Ontology Consortium. Nat Genet *25*, 25-29.
8. Kanehisa, M., Furumichi, M., Tanabe, M., Sato, Y., and Morishima, K. (2017). KEGG: new perspectives on genomes, pathways, diseases and drugs. Nucleic Acids Res *45*, D353-D361.
9. Kumar, P., Henikoff, S., and Ng, P.C. (2009). Predicting the effects of coding non-synonymous variants on protein function using the SIFT algorithm. Nat

Protoc *4*, 1073-1081.

10. Adzhubei, I.A., Schmidt, S., Peshkin, L., Ramensky, V.E., Gerasimova, A., Bork, P., Kondrashov, A.S., and Sunyaev, S.R. (2010). A method and server for predicting damaging missense mutations. Nat Methods *7*, 248-249.
11. Schwarz, J.M., Cooper, D.N., Schuelke, M., and Seelow, D. (2014). MutationTaster2: mutation prediction for the deep-sequencing age. Nat Methods *11*, 361-362.
12. Tang, D., Liu, W., Li, G., He, X., Zhang, Z., Zhang, X., and Cao, Y. (2020). Normal fertility with deletion of sY84 and sY86 in AZFa region. Andrology *8*, 332-336.
13. Wang, Y., Yang, J., Jia, Y., Xiong, C., Meng, T., Guan, H., Xia, W., Ding, M., and Yuchi, M. (2014). Variability in the morphologic assessment of human sperm: use of the strict criteria recommended by the World Health Organization in 2010. Fertil Steril *101*, 945-949.
14. Toyoda, Y., Yokoyama, M., and Hosi, T. (1971). Studies on the fertilization of mouse eggs in vitro I: In vitro fertilization of eggs by fresh epididymal sperm. Jap J Anim Reprod *16*, 147-151.
15. Liu, C., Lv, M., He, X., Zhu, Y., Amiri-Yekta, A., Li, W., Wu, H., Kherraf, Z.E., Liu, W., Zhang, J., et al. (2020). Homozygous mutations in SPEF2 induce multiple morphological abnormalities of the sperm flagella and male infertility. J Med Genet *57*, 31-37.
16. Shimada, K., Kato, H., Miyata, H., and Ikawa, M. (2019). Glycerol kinase 2 is essential for proper arrangement of crescent-like mitochondria to form the mitochondrial sheath during mouse spermatogenesis. J Reprod Dev *65*, 155-162.
17. Cong, L., Ran, F.A., Cox, D., Lin, S., Barretto, R., Habib, N., Hsu, P.D., Wu, X., Jiang, W., Marraffini, L.A., et al. (2013). Multiplex genome engineering using CRISPR/Cas systems. Science *339*, 819-823.
18. Mashiko, D., Fujihara, Y., Satouh, Y., Miyata, H., Isotani, A., and Ikawa, M. (2013). Generation of mutant mice by pronuclear injection of circular plasmid expressing

Cas9 and single guided RNA. Sci Rep *3*, 3355.

19. Abbasi, F., Miyata, H., Shimada, K., Morohoshi, A., Nozawa, K., Matsumura, T., Xu, Z., Pratiwi, P., and Ikawa, M. (2018). RSPH6A is required for sperm flagellum formation and male fertility in mice. J Cell Sci *131*, jcs.221648.
20. Ho, Y., Wigglesworth, K., Eppig, J.J., and Schultz, R.M. (1995). Preimplantation development of mouse embryos in KSOM: augmentation by amino acids and analysis of gene expression. Mol Reprod Dev *41*, 232-238.
21. Ikawa, M., Tokuhiro, K., Yamaguchi, R., Benham, A.M., Tamura, T., Wada, I., Satouh, Y., Inoue, N., and Okabe, M. (2011). Calsperin is a testis-specific chaperone required for sperm fertility. J Biol Chem *286*, 5639-5646.